

OCT 12 1981

AEDC-TR-81-21

C2

*[Handwritten signature]*



# Infrared Reflectance and Refractive Index Measurements in Vacuum-Rated Hemiellipsoidal Mirror Reflectometer from 20 to 300°K

B. E. Wood and A. M. Smith  
ARO, Inc.

September 1981

Interim Report for Period February 1, 1977 — March 1, 1979

Approved for public release, distribution unlimited.

Property of Air Force  
AEDC LIBRARY  
F40600-81-C-0004

**ARNOLD ENGINEERING DEVELOPMENT CENTER  
ARNOLD AIR FORCE STATION, TENNESSEE  
AIR FORCE SYSTEMS COMMAND  
UNITED STATES AIR FORCE**

## NOTICES

When U. S. Government drawings, specifications, or other data are used for any purpose other than a definitely related Government procurement operation, the Government thereby incurs no responsibility nor any obligation whatsoever, and the fact that the Government may have formulated, furnished, or in any way supplied the said drawings, specifications, or other data, is not to be regarded by implication or otherwise, or in any manner licensing the holder or any other person or corporation, or conveying any rights or permission to manufacture, use, or sell any patented invention that may in any way be related thereto.

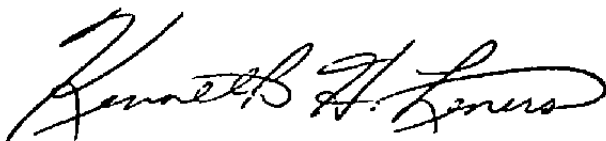
Qualified users may obtain copies of this report from the Defense Technical Information Center.

References to named commercial products in this report are not to be considered in any sense as an indorsement of the product by the United States Air Force or the Government.

This report has been reviewed by the Office of Public Affairs (PA) and is releasable to the National Technical Information Service (NTIS). At NTIS, it will be available to the general public, including foreign nations.

## APPROVAL STATEMENT

This report has been reviewed and approved.



KENNETH H. LENERS, Captain, USAF  
Directorate of Technology  
Deputy for Operations

Approved for publication:

FOR THE COMMANDER



MARION L. LASTER  
Director of Technology  
Deputy for Operations

# UNCLASSIFIED

REPORT DOCUMENTATION PAGE		READ INSTRUCTIONS BEFORE COMPLETING FORM
1 REPORT NUMBER AEDC-TR-81-21	2 GOVT ACCESSION NO.	3 RECIPIENT'S CATALOG NUMBER
4 TITLE (and Subtitle) INFRARED REFLECTANCE AND REFRACTIVE INDEX MEASUREMENTS IN VACUUM-RATED HEMI ELLIPSOIDAL MIRROR REFLECTOMETER FROM 20 to 300°K		5 TYPE OF REPORT & PERIOD COVERED Interim Report - February 1, 1977 - March 1, 1979
		6 PERFORMING ORG REPORT NUMBER
7 AUTHOR(s) B. E. Wood and A. M. Smith, ARO, Inc., a Sverdrup Corporation Company		8 CONTRACT OR GRANT NUMBER(s)
9 PERFORMING ORGANIZATION NAME AND ADDRESS Arnold Engineering Development Center/DOT Air Force Systems Command Arnold Air Force Station, Tennessee 37389		10 PROGRAM ELEMENT, PROJECT, TASK AREA & WORK UNIT NUMBERS Program Element 65807F
11 CONTROLLING OFFICE NAME AND ADDRESS Arnold Engineering Development Center/DOS Air Force Systems Command Arnold Air Force Station, Tennessee 37389		12 REPORT DATE September 1981
		13 NUMBER OF PAGES 35
14 MONITORING AGENCY NAME & ADDRESS (if different from Controlling Office)		15 SECURITY CLASS (of this report) UNCLASSIFIED
		15a DECLASSIFICATION/DOWNGRADING SCHEDULE N/A
16 DISTRIBUTION STATEMENT (of this Report)  Approved for public release; distribution unlimited.		
17 DISTRIBUTION STATEMENT (of the abstract entered in Block 20, if different from Report)		
18 SUPPLEMENTARY NOTES  Available in Defense Technical Information Center (DTIC)		
19 KEY WORDS (Continue on reverse side if necessary and identify by block number) <div style="display: flex; flex-wrap: wrap;"> <div style="width: 33%;">ellipsoids</div> <div style="width: 33%;">surfaces</div> <div style="width: 33%;">chemicals</div> <div style="width: 33%;">mirrors</div> <div style="width: 33%;">condensation</div> <div style="width: 33%;">etching</div> <div style="width: 33%;">reflectometers</div> <div style="width: 33%;">thin films</div> <div style="width: 33%;">salts</div> <div style="width: 33%;">cryogenics</div> <div style="width: 33%;">gases</div> <div style="width: 33%;">reflectance</div> <div style="width: 33%;">optics</div> <div style="width: 33%;">anodic coatings</div> <div style="width: 33%;">refractive index</div> </div>		
20 ABSTRACT (Continue on reverse side if necessary and identify by block number)  Experimental studies have been carried out for determining the change in reflectance caused by the condensation of thin films on 77 and 20°K mirror surfaces in the 2- to 25-μm wavelength range. Refractive indices of the gases condensed were measured at the He-Ne laser wavelength, 0.6328 μm. Hemispherical-directional reflectance measurements of the mirror-condensed gas composites were made using a hemiellipsoidal mirror reflectometer system. The		

# UNCLASSIFIED

# UNCLASSIFIED

## 20. ABSTRACT (Continued)

refractive index and reflectance of condensed films of  $N_2$ ,  $O_2$ ,  $CO_2$ ,  $H_2O$ ,  $NH_3$ ,  $N_2O$ ,  $NO$ ,  $CO$ ,  $CH_4$ , argon, air, and allene were measured. Thicknesses and refractive indices were determined using the two-angle interference technique. In addition to the reflectance measurements made on cryogenic samples, an interfascility comparison of reflectance measurements was made on several anodized metal coatings at room temperature using reflectometers at the Air Force Materials Laboratory at Wright-Patterson Air Force Base, the Convair Division of General Dynamics Corporation in San Diego, and at AEDC. Reflectance measurements were also made on a variety of salt samples (such as nitrates, sulfates, and chlorides) at room temperature and at 77°K to demonstrate the applications available for the HEMR.

## **PREFACE**

The work reported herein was conducted by the Arnold Engineering Development Center (AEDC), Air Force Systems Command (AFSC). The research results were obtained by ARO, Inc., AEDC Division (a Sverdrup Corporation Company), operating contractor for the AEDC, AFSC, Arnold Air Force Station, Tennessee. The research was done under ARO Project No. V32K-13A. The manuscript was submitted for publication on April 9, 1979.

The authors would like to express their gratitude to the following ARO personnel who assisted in the design of some of the components: J. G. Pipes, J. W. Richardson, L. D. Sanders, S. D. Forbord, S. G. Ansley, and F. G. Sherrill, and to J. A. Roux for technical suggestions and comments during this investigation.

Mr. B. E. Wood is currently employed by Calspan Field Services, Inc./AEDC Division, while Dr. A. M. Smith is the Dean of Engineering at the University of Mississippi.

## CONTENTS

	<u>Page</u>
1.0 INTRODUCTION .....	5
2.0 DESCRIPTION OF HEMR .....	6
3.0 APPARATUS .....	7
4.0 REFRACTIVE INDICES OF CONDENSED GASES .....	10
5.0 SPECTRAL REFLECTANCE MEASUREMENTS OF CONDENSED GASES ...	14
6.0 COMPARISON OF REFLECTANCE MEASUREMENTS .....	21
7.0 SUMMARY .....	27
REFERENCES .....	28

## ILLUSTRATIONS

### Figure

1. Hemiellipsoidal Mirror Reflectometer System .....	6
2. Components of HEMR System .....	7
3. Double-Angle Laser Interference System .....	9
4. Two-Angle Interference Techniques .....	11
5. Reflectance of CO <sub>2</sub> Film on 77°K Aluminum Mirror .....	15
6. Reflectance of H <sub>2</sub> O Film on 77°K Aluminum Mirror .....	16
7. Reflectance of Ammonia Film on 77°K Aluminum Mirror .....	16
8. Reflectance of CO Film on 20°K Aluminum Mirror .....	17
9. Reflectance of CH <sub>4</sub> Film on 20°K Aluminum Mirror .....	18
10. Reflectance of N <sub>2</sub> O Film on 20°K Aluminum Mirror .....	18
11. Reflectance of NO Film on 20°K Aluminum Mirror .....	19
12. Reflectance of Condensed Air Film on 20°K Aluminum Mirror .....	20
13. Reflectance of Condensed Allene Film on 20°K Aluminum Mirror .....	20
14. Comparison of Reflectance Data from GDC, AFML, and AEDC for a 6061 Aluminum Sample That was H <sub>2</sub> SO <sub>4</sub> Anodized by Anodite, Inc. ....	22
15. Comparison of Reflectance Data from GDC, AFML, and AEDC for a 6061 Aluminum Sample That was Deep Chemically Etched and H <sub>2</sub> SO <sub>4</sub> Anodized by Anodite, Inc. ....	23
16. Comparison of Reflectance Data from GDC, AFML, and AEDC for a 6061 Sample That was Anodized by Hardes, Inc. ....	23

<u>Figure</u>	<u>Page</u>
17. Comparison of Reflectance Data from AFML and AEDC for a 6061 Aluminum Sample That was H <sub>2</sub> SO <sub>4</sub> Anodized at AEDC .....	23
18. Comparison of Reflectance Data from GDC, AFML, and AEDC for a 7075 Aluminum Sample That was H <sub>2</sub> SO <sub>4</sub> Anodized by Anodite, Inc. ....	23
19. Comparison of Reflectance Data from GDC, AFML, and AEDC for a 7075 Aluminum Sample That was Anodized by Hardes, Inc. ....	24
20. Comparison of Reflectance Data from GDC, AFML, and AEDC for a 7075 Aluminum Sample That was Deep Chemically Etched and H <sub>2</sub> SO <sub>4</sub> Anodized by Anodite, Inc. ....	24
21. Comparison of Reflectance Data from GDC, AFML, and AEDC for a 2024 Aluminum Sample That was Deep Chemically Etched and H <sub>2</sub> SO <sub>4</sub> Anodized by Anodite, Inc. ....	24
22. Comparison of Reflectance Data from GDC, AFML, and AEDC for a 2024 Aluminum Sample That was Anodized by Hardes, Inc. ....	24
23. Comparison of Reflectance Data from GDC, AFML, and AEDC for a Titanium Sample That was Anodized by Anodite, Inc. ....	25
24. Comparison of Reflectance Data from GDC, AFML, and AEDC for a Titanium Sample That was Anodized by Lubeco, Inc. ....	25
25. Comparison of Reflectance Data from GDC, AFML, and AEDC for a Beryllium Sample That was Anodized by Anodite, Inc. ....	26
26. Comparison of Reflectance of Optosil I Measured in the HEMR at AEDC with the Results of the General Dynamics Convair Reflectometer .....	26
27. Comparison of HEMR Reflectance Measurements for Bendix Black Paint Sample #1601 Krylon® with Those Obtained at NBS .....	27

## TABLES

1. Refractive Indices (at $\lambda = 0.6328 \mu\text{m}$ ) and Deposition Conditions for Condensed Gases on 77 and 20°K Aluminum Mirrors .....	13
2. SAMSO Anodized Samples .....	22

## APPENDIX

A. REFLECTANCE MEASUREMENTS OF POSSIBLE PLANETARY SATELLITE SURFACE CONSTITUENTS .....	31
---	----

## 1.0 INTRODUCTION

The hemiellipsoidal mirror reflectometer (HEMR) is described in Refs. 1 and 2 for a bench-type operation for samples at ambient temperature and pressure. This report describes the HEMR and its operation in vacuum for cryogenically cooled samples. As described in Ref. 1, the HEMR has a wavelength-range capability from 2 to 34  $\mu\text{m}$  in its present configuration, but, with some modifications, this could be extended to shorter or longer wavelengths. The range from 2 to 34  $\mu\text{m}$  covers the important region for species identification since most of the vibration-rotation absorption bands occur in this wavelength band.

The effects of condensed gases on surface reflectance have received much investigation over the years. Reflectance effects of  $\text{H}_2\text{O}$  and  $\text{CO}_2$  condensed on surfaces have been studied for solar and infrared (IR) ranges. (Refs. 3, 4, 5, 6, and 7). The effects of condensed gases on the directional distribution of radiation reflected from specular and nonspecular surfaces have also been studied (Refs. 8, 9, 10, and 11). In this investigation thin films of condensed gases were formed on mirror surfaces and the hemispherical-directional reflectance measured as a function of wavelength from 2 to 25  $\mu\text{m}$ . The refractive index of each gas was measured in situ, allowing accurate film thicknesses to be calculated from thin-film interference patterns. The condensed gas properties were studied to determine the optical effects of different gases condensed on critical optical surfaces. These situations arise in test facilities such as sensor testing chambers or in actual satellite flight. In ground test facilities, these contaminant gases are present due to outgassing from materials and atmospheric leaks. Space contamination is generally caused by gases from thrusters, cooling systems, or material outgassing products. The gases studied in this report were  $\text{CO}_2$ ,  $\text{H}_2\text{O}$ ,  $\text{NH}_3$ ,  $\text{CO}$ ,  $\text{N}_2$ ,  $\text{O}_2$ ,  $\text{CH}_4$ ,  $\text{NO}$ ,  $\text{N}_2\text{O}$ , allene ( $\text{C}_3\text{H}_4$ ), argon, and air. Most of these gases are common atmospheric or rocket engine exhaust gases and, thus, are of concern as optical surface contaminants.

In this report reflectance measurements are presented for basically three different scopes of interest. The primary emphasis was on the determination of the reflectance and refractive index of thin films ( $\approx 10 \mu\text{m}$  thick) of various gases condensed on cryogenically cooled plane metal mirrors in vacuum. Another emphasis was the interfacility comparison of reflectance measurements on anodized samples, wherein comparisons of measurements at the Convair Division of General Dynamics in San Diego, at the Air Force Materials Laboratory at Wright-Patterson Air Force Base, and at AEDC were made. This provided an excellent chance to determine the measurement agreement among the different types of instruments. The third effort consisted of making reflectance measurements on chemical



sulfates and carbonates at room temperature and at 77°K. These results are given in Appendix A.

## 2.0 DESCRIPTION OF HEMR

In the HEMR the spectral hemispherical-directional reflectance is the property measured. As discussed in Ref. 1, the hemispherical-directional reflectance,  $\rho_{hd,s}$ , is determined from

$$\rho_{hd,s}(\lambda) = \frac{B_s(\lambda)}{B_{ref}(\lambda)} \quad (1)$$

where  $B_s(\lambda)$  is the spectral detector output determined with the spectrometer viewing the sample and  $B_{ref}(\lambda)$  is the detector output obtained when the spectrometer is viewing a gold reference surface that has a reflectance near unity. Reflectance measurements are made by simply ratioing the two detector outputs at a given wavelength  $\lambda$ . All measurements were made for a view angle of 15 deg.

Figures 1 and 2 show schematically the HEMR and associated equipment. The ellipsoidal

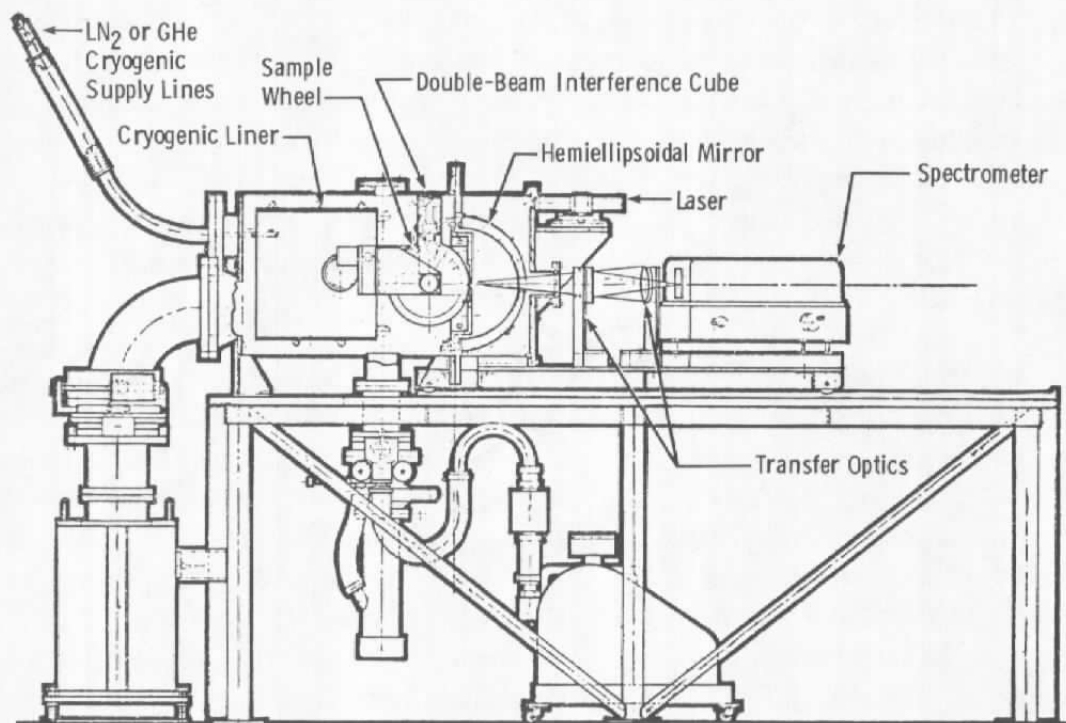


Figure 1. Hemiellipsoidal mirror reflectometer system.

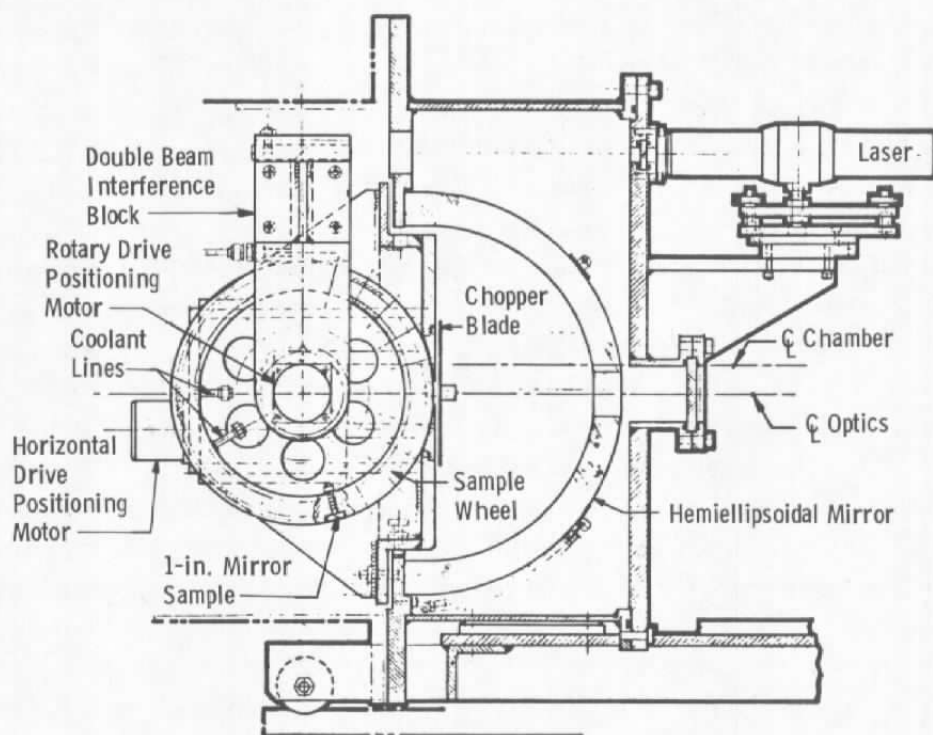


Figure 2. Components of HEMR system.

mirror is approximately 32.48 cm (12 in.) in diameter at the major focal plane. The ellipsoid has a semimajor axis of  $b = 16.24$  cm (6.0 in.) and semiminor axes of  $a = 15.03$  cm (5.916 in.) and is expressed mathematically as

$$\frac{x^2 + z^2}{a^2} + \frac{y^2}{b^2} = \frac{x^2 + z^2}{(5.916)^2} + \frac{y^2}{(6.0)^2} = 1 \quad (2)$$

This ellipsoid has two foci located on the major axis each 2.54 cm (1 in.) away from the original with a 5.08-cm (2 in.) total separation of the foci. The ellipsoid has the property such that an object located at one focus will, in turn, be imaged at the conjugate focus. Locating a diffuse light source at one focus results in the diffuse irradiance of a surface located at the other focus. The operation and basic principles are discussed in Refs. 1 and 2.

### 3.0 APPARATUS

The hemiellipsoidal mirror was obtained commercially. It was made by molding 1.91-cm- (3/4 in.) thick Pyrex® into a hemisphere. The outside diameter was essentially that of a hemisphere 34.3 cm (13.5 in.) in diameter. Grinding and polishing the interior produced the desired configuration and dimensions. The result was a high-quality mirror surface with

a semimajor axis of 16.24 cm (6 in.) and a semiminor axis of 15.03 cm (5.916 in.). The mirror coating was vacuum-deposited aluminum, which has a reflectivity of 97 to 99 percent for the 2- to 35- $\mu$ m wavelength range. A hole 3.81 cm (1.50 in.) in diameter was cut in the mirror to pass radiation reflected from the sample located at one focus out to the spectrometer. The hole was located so that the center corresponded to a reflection angle of  $\theta = 15$  deg.

A commercially built blackbody was used for the radiation source. It was constructed of oxygen-free copper, and the interior had been machined to form a blunt cone. Metal-sheathed electric heating elements were wound around the exterior and brazed to the copper surface with a gold-copper alloy. The cone interior surface was plasma-sprayed with stainless steel, which oxidizes, when heated, to form a high-emittance coating. Normal blackbody operating temperature was 427 to 482°C (800 to 900°F). For operating in vacuum, approximately 30 w of power were required. A water-cooled jacket surrounded the blackbody to prevent heat transfer to other components in the HEMR. The blackbody cavity opening was 2.54 cm (1 in.) in diameter, and the cavity depth was 3.49 cm (1.375 in.), yielding a depth-to-radius ratio (L/R) of 2.75. It was established in Ref. 1 that the blackbody-emitted energy was diffuse; this diffusion was one of the fundamental operating requirements for the HEMR. The blackbody was apertured by an 8- by 30-mm slit to restrict the sample area irradiated so as to minimize the heating errors discussed in Ref. 1. Radiation emitted from the blackbody was modulated at a frequency of 13 Hz, with the polished aluminum chopper blade positioned as close as possible to the blackbody exit plane. Using a chopped signal eliminated the sample self-emission problem present in some types of reflectometers. The spectrometer was a single-pass Perkin-Elmer Model 98 monochromator that used a KBr prism from dispersion and a thermocouple for detection.

The refractive index and thickness monitoring system is depicted in Fig. 3. A 2-mw He-Ne laser beam of 0.6328- $\mu$ m wavelength was passed into the chamber through a small chamber window. The beam was reflected downward toward the sample by a flat mirror. With a beam-splitter cube (15 mm square), the beam was split into two beams; one went directly through the cube and was incident normal to the test surface, and the other beam was directed through the side of the cube, was reflected off another plane mirror, and was incident on the test surface at 45 deg. The beam incident at 45 deg was specularly reflected directly to a silicon solar cell, whereas the normal incident beam was reflected back to the beam splitter, at which point one half retraced the entrance beam and the other half was redirected to another silicon solar cell (see Fig. 3). The solar cell detector outputs were displayed on a strip chart recorder.

The sample wheel (Figs. 1 and 2) was made of aluminum. It had narrow internal passages to allow either liquid nitrogen (LN<sub>2</sub>) or gaseous helium (GHe) cryogenic cooling. The sample

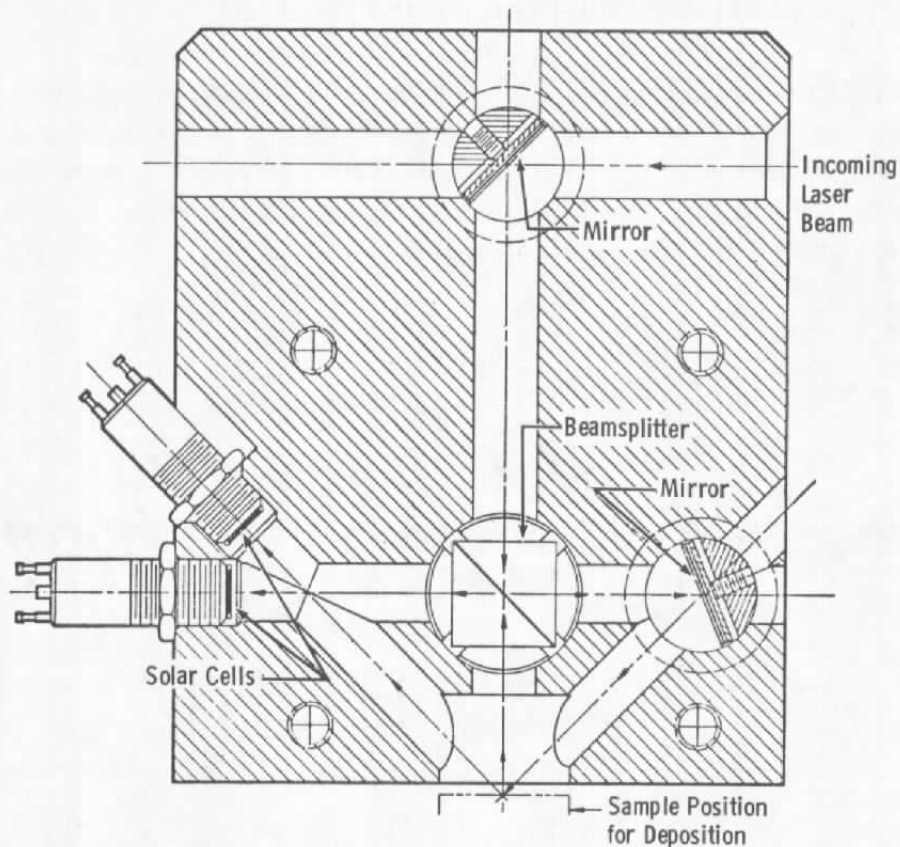


**Figure 3. Double-angle laser interference system.**

positions were machined into the sample wheel to allow the location of eight sample surfaces that were 2.54 cm (1 in.) in diameter and 0.635 cm (0.25 in.) thick. The samples used in this investigation were solid aluminum mirrors polished to attain a highly specular surface. The mirror surfaces that had been drilled and tapped through their rear surfaces were attached to the wheel by locking each one down with a spring washer and nut (see Fig. 2) and using a thin washer of indium to ensure good thermal contact. Location of the samples at the mirror foci was achieved through two positioning stepper motors: one for rotary motion and the other for lateral movement into and out of the ellipsoid. Lateral movement in steps of 0.0025 cm (0.001 in.) was obtained to position the sample accurately at the mirror focus. Seven of the eight sample positions achieved the same temperature as the sample wheel. The remaining sample was isolated thermally from the sample wheel to keep a clean, gold reference mirror at or near room temperature and free of any condensed gases. This allowed the gold reference measurements to be made at any time during the experiment.

#### 4.0 REFRACTIVE INDICES OF CONDENSED GASES

Refractive index measurements of gases condensed on specular surfaces were made using the two-angle interference technique. This technique is discussed in detail in Ref. 12 and is depicted in Fig. 4. The detector output varies sinusoidally as the film is being condensed on the substrate because of thin-film interference. The thickness of the deposit,  $\tau$ , can be determined at any interference maxima or minima from

$$\tau = m\lambda / \left[ 2n \left( 1 - \sin^2 \psi / n^2 \right)^{1/2} \right] \quad (3)$$

where  $m = 1, 2, 3, \dots$  for maxima, and

$$\tau = (m + 1/2) \lambda / \left[ 2n \left( 1 - \sin^2 \psi / n^2 \right)^{1/2} \right] \quad (4)$$

where  $m = 0, 1, 2, 3, \dots$  for minima. For radiation incident on the substrate at two angles  $\psi_1$  and  $\psi_2$ , the refractive index can be determined (Ref. 12) from

$$n = \left[ \frac{\sin^2 \psi_2 - \left( \frac{\Delta t_1}{\Delta t_2} \right)^2 \sin^2 \psi_1}{1 - \left( \frac{\Delta t_1}{\Delta t_2} \right)^2} \right]^{1/2} \quad (5)$$

where  $\Delta t_1$  and  $\Delta t_2$  are the periods of the interference minima or maxima for the incident angles  $\psi_1$  and  $\psi_2$ , respectively. Equation (5) is arrived at by assuming that the deposition rate,  $\dot{\tau}$ , is a constant. A similar expression can be obtained by counting the number of maxima or minima obtained over a given time interval (or thickness) for each angle where the patterns are being monitored simultaneously. In this case the thickness,  $\tau$ , is the same, and

$$\tau = \frac{m_1 \lambda}{2n \sqrt{1 - \sin^2 \psi_1 / n^2}} = \frac{m_2 \lambda}{2n \sqrt{1 - \sin^2 \psi_2 / n^2}} \quad (6)$$

Solving for  $n$  yields

$$n = \sqrt{\frac{\sin^2 \psi_1 - \left( \frac{m_1}{m_2} \right)^2 \sin^2 \psi_2}{1 - \left( \frac{m_1}{m_2} \right)^2}} \quad (7)$$

$$\frac{\Delta \tau}{\Delta t_{1,2}} = \tau = \text{Constant} = \frac{(\Delta m) \lambda}{2n \sqrt{1 - \frac{\sin^2 \psi_1}{n^2}}} = \frac{(\Delta m) \lambda}{2n \sqrt{1 - \frac{\sin^2 \psi_2}{n^2}}}$$

or

$$n = \frac{\sqrt{\sin^2 \psi_2 - \left(\frac{\Delta t_1}{\Delta t_2}\right)^2 \sin^2 \psi_1}}{\sqrt{1 - \left(\frac{\Delta t_1}{\Delta t_2}\right)^2}}$$

a) Constant Deposition Rate Required for Both Angles

$$\tau = \frac{m_1 \lambda}{2n \sqrt{1 - \frac{\sin^2 \psi_1}{n^2}}} = \frac{m_2 \lambda}{2n \sqrt{1 - \frac{\sin^2 \psi_2}{n^2}}}$$

or

$$n = \frac{\sqrt{\sin^2 \psi_1 - \left(\frac{m_1}{m_2}\right)^2 \sin^2 \psi_2}}{\sqrt{1 - \left(\frac{m_1}{m_2}\right)^2}}$$

b) Equal Change in Thickness Required for Both Angles

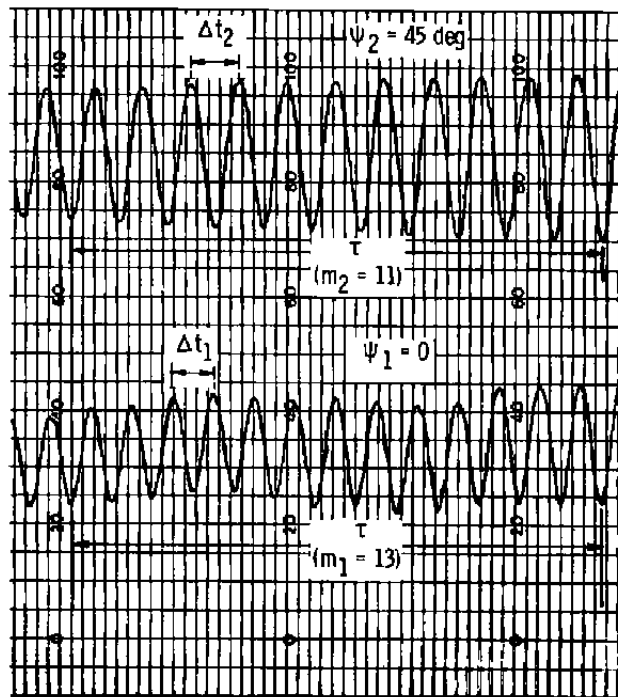


Figure 4. Two-angle interference techniques.

The major difference between the two techniques is that Eq. (5) does not require that the patterns be measured simultaneously but does require a constant deposition rate. For Eq. (7), the patterns have to be measured simultaneously for the same deposit thickness, but the deposition rate does not have to be constant.

The experimental components required for the refractive index measurements have been discussed in Section 3.0. The two incident angles  $\psi_1$  and  $\psi_2$  were arranged to be 0 and 45 deg, respectively. It was desired to have  $\psi_2$  as large as possible to yield a smaller ratio of  $(\Delta t_1/\Delta t_2)$  and hence a larger value of the term  $[1 - (\Delta t_1/\Delta t_2)^2]$  in the denominator of Eq. (5). If  $\Delta t_1$  and  $\Delta t_2$  are nearly equal, then the small number in the denominator increases the uncertainty involved, because of division by a very small number. Similar arguments can be made that the Eq. (7) ratio of  $(m_1/m_2)$  should be as large as possible to maximize the absolute value in the denominator.

The refractive index ( $\lambda = 0.6328 \mu\text{m}$ ) of the various gases studied and the condensation conditions of deposition pressure, substrate temperature, and deposition rate are presented in Table 1. All of the gases except  $\text{H}_2\text{O}$  and air were compressed gases. For the  $\text{H}_2\text{O}$  measurements a special water-gas addition system was used. Distilled  $\text{H}_2\text{O}$  was first purified under vacuum and then allowed to evaporate and pass through a metering valve into the chamber. Over the range of deposition rates (Table 1) 0.09 to  $3.9 \mu\text{m}/\text{min}$ , no significant change in refractive index was noted, although this entire range of deposition rates was not covered for each gas. For the gases that will condense on both  $\text{LN}_2$ - and  $\text{GHe}$ -cooled surfaces, the refractive index decreases with decreasing substrate temperature. This indicates also that the deposits are less dense at the lower temperatures, a fact that has been proved in other similar experiments at AEDC using a quartz crystal microbalance (QCM). For the Lorentz-Lorenz formula

$$\left( \frac{n^2 - 1}{n^2 + 2} \right) \cdot \frac{1}{D} = P(\lambda)$$

it is found that for decreasing  $n$ , the density  $D$  also must decrease, since the specific refractive  $P(\lambda)$  is a constant at a given wavelength for a given material regardless of its solid, liquid, or gaseous state.

For each gas listed in Table 1, the refractive index shown is an average of 5 to 10 individual measurements for that particular condensed gas. The rotary wheel contained the seven mirror samples that could be cooled simultaneously. By positioning each sample at the point of deposition, several determinations of  $n$  could be made during a single pumpdown. The refractive indices listed in Table 1 were generally within uncertainty bands of  $\pm 0.01$  with a maximum variation of  $\pm 0.02$  for most of the gases. For  $\text{NO}$  the uncertainty band is given as  $\pm 0.02$ , but this was believed to be due to  $\text{NO}_2$  impurities since  $\text{NO}$  readily oxidizes

**Table 1. Refractive Indices (at  $\lambda = 0.6328 \mu\text{m}$ ) and Deposition Conditions for Condensed Gases on 77 and 20°K Aluminum Mirrors**

Gas	Refractive index at 77°K	Refractive index at 20°K	Deposition pressure, Torr		Deposition rate, $\mu\text{m/min}$	
			Substrate temp. = 77°K	Substrate temp. = 20°K	Substrate temp. = 77°K	Substrate temp. = 20°K
Carbon dioxide ( $\text{CO}_2$ )	$1.43 \pm 0.01$	$1.28 \pm 0.01$	$4-8 \times 10^{-7}$	$4 \times 10^{-8}$	$0.98 - 1.85$	$0.85 - 0.95$
Water ( $\text{H}_2\text{O}$ )	$1.31 \pm 0.01$	$1.28 \pm 0.01$	$2 \times 10^{-6}$	$2-5 \times 10^{-8}$	$0.09 - 1.25$	$0.09 - 1.23$
Ammonia ( $\text{NH}_3$ )	$1.42 \pm 0.01$	$1.37 \pm 0.01$	$2-6 \times 10^{-6}$	$4 \times 10^{-8}$	$0.5 - 0.7$	$0.7$
Carbon monoxide ( $\text{CO}$ )	---	$1.30 \pm 0.01$	---	$4-6 \times 10^{-8}$	---	$0.95 - 1.72$
Methane ( $\text{CH}_4$ )	---	$1.36 \pm 0.01$	---	$2-4 \times 10^{-8}$	---	$0.8 - 3.4$
Oxygen ( $\text{O}_2$ )	---	$1.31 \pm 0.01$	---	$4.5 \times 10^{-8}$	---	$0.7 - 1.35$
Nitrogen ( $\text{N}_2$ )	---	$1.28 \pm 0.01$	---	$2.5-3 \times 10^{-8}$	---	$1.71 - 1.74$
Argon (A)	---	$1.31 \pm 0.01$	---	$2-5 \times 10^{-8}$	---	$0.67 - 1.20$
Air	---	$1.28 \pm 0.01$	---	$3-8 \times 10^{-8}$	---	$1.6 - 1.7$
Nitric oxide ( $\text{NO}$ )	---	$1.38 \pm 0.02$	---	$4 \times 10^{-8}$	---	$0.95 - 1.08$
Nitrous oxide ( $\text{N}_2\text{O}$ )	---	$1.29 \pm 0.01$	---	$7 \times 10^{-8}$	---	$2.21$
Allene ( $\text{C}_3\text{H}_4$ )	$1.43 \pm 0.02$	$1.26 \pm 0.01$	$2 \times 10^{-6}$	$4-8 \times 10^{-8}$	$3.6 - 3.9$	$3.6 - 3.9$

to  $\text{NO}_2$ . Occasional anomalous variations were noted for ammonia, but these were believed to be due to different phases of deposit. Usually the interference patterns lasted considerably longer for the higher incidence angle ( $\psi = 45^\circ$ ), but for allene and  $\text{NO}$ , the patterns were unusual. The patterns for  $\psi = 0$  would decrease in intensity, die out completely, and then begin to increase again. When this occurred, the patterns for  $\psi = 45^\circ$  would die out completely before those for  $\psi = 0$ , just opposite the normal behavior of the other condensed gases. This phenomenon is as yet unexplained.



Refractive index measurements of some condensed gases have been reported previously in Refs. 7, 12, 13, and 14. The data for CO<sub>2</sub> show agreement between all studies for the 77°K refractive index measurement,  $1.43 \pm 0.01$  at  $0.6328 \mu\text{m}$ . The value of  $1.28 \pm 0.01$  for the 20°K CO<sub>2</sub> measurements disagrees with the 1.34 value of Ref. 7 and is considerably lower than the 1.42 value of Ref. 14. For H<sub>2</sub>O at 77°K, the value of  $1.31 \pm 0.01$  approximates Ref. 7 (1.32) but is considerably higher than the value of 1.26 of Refs. 13 and 14. This is believed to be due to the deposition of the films of the present study at a chamber pressure of  $10^7 - 10^8$  torr, whereas the films of Ref. 13 were deposited at a pressure of  $10^4 - 10^3$  torr. At this higher deposition pressure, there is an increased likelihood of voids or of N<sub>2</sub> trapping that tends to decrease the refractive index. Undoubtedly, the deposition pressure can have a significant effect on the refractive index and density of the deposited films. The refractive index  $1.42 \pm 0.01$  measured for ammonia at 77°K agrees well with Refs. 7 and 14, but the value of  $1.37 \pm 0.01$  at 20°K disagrees with the 1.42 value of Ref. 14. However, it nearly agrees with the value of 1.38 of Ref. 7. The value of CH<sub>4</sub> of  $1.36 \pm 0.01$  is close to the value of 1.38 of Ref. 14. The oxygen refractive index of  $1.31 \pm 0.01$  is the same as that observed in Ref. 7. However, the value for N<sub>2</sub> of  $1.28 \pm 0.01$  is above the value of 1.24 observed in Ref. 7.

## 5.0 SPECTRAL REFLECTANCE MEASUREMENTS OF CONDENSED GASES

The procedure for making reflectance measurements in the HEMR under vacuum conditions was similar in principle to that of Ref. 1 for measurements on room-temperature surfaces at atmospheric pressures. The blackbody source was allowed to reach operating temperature ( $\approx 900^\circ\text{F}$  or  $482^\circ\text{C}$ ) before cryogenically cooling the sample mirrors. This procedure removed blackbody outgassing products from the HEMR system, thus preventing any possibility of their condensation on the sample surface when it was cooled cryogenically. The gold reference surface was isolated thermally from the cryogenically cooled sample wheel and remained at our near room temperature. This eliminated the possibility of condensation of gases on the reference surface.

The sample wheel — at either 77 or 20°K — was positioned such that the aluminum mirror of interest was located at the gas deposition location. This was established by monitoring the solar cell outputs for the laser beam at normal incidence and at 45 deg to the test mirror. The test gas flow was started, and the interference patterns were recorded. As the refractive index had been measured previously, a desired thickness was obtained by counting the interference maxima or minima. The gas flow was shut off when the thin-film thickness reached about  $10 \mu\text{m}$ , as determined from the interference patterns. Spectral reflectance measurements were made by rotating the sample mirror coated with the condensed test gas to the sample foci of the mirror. Reflectance spectra were recorded for both the sample and the gold, room-temperature mirror, and ratios were determined. In this manner the spectral reflectance of the condensed test gas on the mirror was determined.

Figures 5 to 13 show spectral reflectance for the following condensed gases:  $\text{CO}_2$ ,  $\text{H}_2\text{O}$ ,  $\text{NH}_3$  (all at 77°K), and  $\text{CO}$ ,  $\text{CH}_4$ ,  $\text{N}_2\text{O}$ ,  $\text{NO}$ , air, and allene (all at 20°K). The deposition pressure or chamber pressure was routinely  $2$  to  $5 \times 10^{-7}$  torr for 77°K temperature surfaces and  $3$  to  $5 \times 10^{-8}$  torr for gases deposited on the 20°K surfaces. The cryogenic liner inside the chamber was always at the same temperature as the sample wheel and helped keep the chamber pressure low during depositions. Also, the diffusion pump was always left on during deposition to help remove noncondensables, especially for the 77°K measurements.

### Carbon Dioxide ( $\text{CO}_2$ )

Figure 5 shows the reflectance of a 10.2- $\mu\text{m}$ -thick  $\text{CO}_2$  film condensed on an aluminum mirror substrate at 77°K. The refractive indices for  $\text{CO}_2$  at  $\lambda = 0.6328 \mu\text{m}$  were  $1.43 \pm 0.01$  at 77°K and  $1.28 \pm 0.01$  at 20°K. The three main wavelength regions in which absorption occurs are (in order of intensity) the 4.1- to 4.3- $\mu\text{m}$   $\nu_3$  fundamental band, the  $\nu_2$  fundamental band located at 15.0 to 16.0  $\mu\text{m}$ , and the  $\nu_2 + \nu_3$  combination band located at 2.8 to 2.9  $\mu\text{m}$ . The channel spectra oscillations (interference patterns) can be observed in the 5- to 10- $\mu\text{m}$  wavelength range.

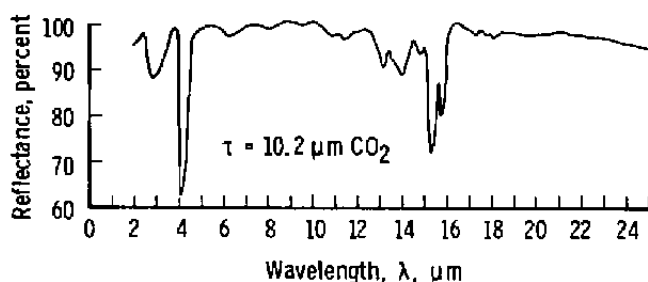
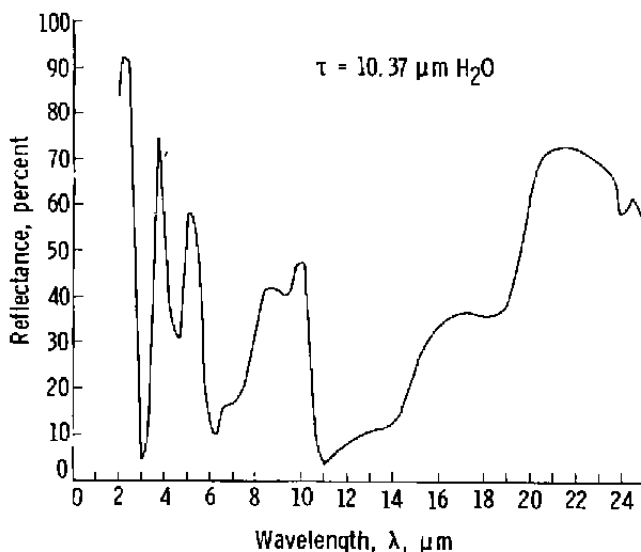


Figure 5. Reflectance of  $\text{CO}_2$  film on 77°K aluminum mirror.

### Water ( $\text{H}_2\text{O}$ )

Reflectance measurements of a 10.37- $\mu\text{m}$ -thick film of  $\text{H}_2\text{O}$  formed on an aluminum mirror (at 77°K) are shown in Fig. 6. There is considerable absorption in the infrared. The major areas of absorption are (1) the band centered around 3.0  $\mu\text{m}$ , due to the  $\nu_1$  and  $\nu_3$  fundamental bands and combinations, (2) the band at approximately 4.7  $\mu\text{m}$ , which is the  $\nu_2 + \nu_L$  combination band, (3) the 6.2- $\mu\text{m}$  band, which is the  $\nu_2$  fundamental, (4) the libration band  $\nu_L$  between 11 and 14  $\mu\text{m}$ , and (5) a rotational band about 19  $\mu\text{m}$ . In general, the  $\text{H}_2\text{O}$  film, when deposited at 77°K, shattered after a thickness of only 6 to 8 interference maxima. After changing the mirror temperature to about 120°K, no problem was encountered in depositing the films. The reflectance data in Fig. 6 are for a deposit formed at 120°K and then cooled down to 77°K without shattering occurring. In some instances the entire film



**Figure 6. Reflectance of  $\text{H}_2\text{O}$  film on  $77^\circ\text{K}$  aluminum mirror.**

left the surface during this shattering phenomenon, whereas at other times the film just shattered or cracked in many directions. This shattering phenomenon is not the same as the amorphous-to-crystalline-phase change observed previously for  $\text{H}_2\text{O}$  deposits (Ref. 4). The refractive indices for solid  $\text{H}_2\text{O}$  at  $\lambda = 0.6328 \mu\text{m}$  for  $77$  to  $20^\circ\text{K}$  were  $1.31 \pm 0.01$  and  $1.28 \pm 0.01$ , respectively.

### **Ammonia ( $\text{NH}_3$ )**

An ammonia film  $9.6 \mu\text{m}$  thick was formed on a  $77^\circ\text{K}$  aluminum mirror, and the reflectance of the combination is shown in Fig. 7. The  $\nu_3$  band is seen at a wavelength of

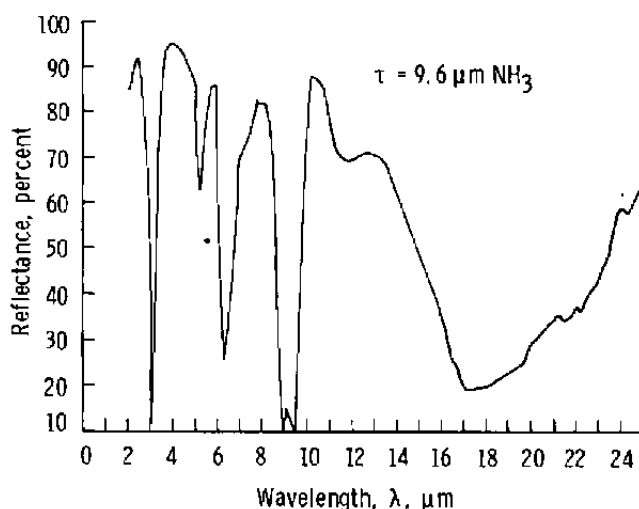


**Figure 7. Reflectance of ammonia film on  $77^\circ\text{K}$  aluminum mirror.**

about  $3.1\text{ }\mu\text{m}$ , the  $\nu_4$  band at  $6.3\text{ }\mu\text{m}$ , and the  $\nu_2$  band between  $9$  and  $10\text{ }\mu\text{m}$ . In addition to these fundamentals, absorption bands are seen at  $5.3\text{ }\mu\text{m}$  and at approximately  $11.8\text{ }\mu\text{m}$ , and there is also a very broad region of absorption around  $18.5\text{ }\mu\text{m}$ . Refractive indices at  $\lambda = 0.6328\text{ }\mu\text{m}$  for solid  $\text{NH}_3$  at  $77$  and  $20^\circ\text{K}$  were found to be, respectively,  $1.42 \pm 0.01$  and  $1.37 \pm 0.01$ . Twice, at  $77^\circ\text{K}$ , refractive index values of  $1.51$  were obtained. These values were real and indicative of a different phase of the deposit.

### Carbon Monoxide (CO)

The other gases studied were condensed on  $20^\circ\text{K}$  surfaces (gaseous helium cooled) and, in most instances, would not have condensed on  $77^\circ\text{K}$  surfaces at the chamber pressure ( $\approx 10^{-8}$  torr) at which the films were deposited. Figure 8 shows the reflectance of an  $11.4\text{-}\mu\text{m}$ -thick CO film condensed on an aluminum mirror. The two bands that show up are at  $\lambda = 2.9$  and  $4.5\text{ }\mu\text{m}$ . The band at  $2.9\text{ }\mu\text{m}$ , however, is not due to CO but is due to a trace of water. As was observed in the data for  $\text{H}_2\text{O}$  in Fig. 6,  $\text{H}_2\text{O}$  has a strong absorption band in the  $2.9$ -to  $3.0\text{-}\mu\text{m}$  region. The origin of the  $\text{H}_2\text{O}$  is unknown, but the  $\text{H}_2\text{O}$  did show up in this spectrum and in some of the spectra remaining to be discussed. The CO band located at  $4.5\text{ }\mu\text{m}$  is the fundamental stretching mode and is the only infrared band of any consequence. The solid CO refractive index at  $\lambda = 0.6328\text{ }\mu\text{m}$  was measured and found to be  $1.30 \pm 0.01$  at  $20^\circ\text{K}$ .

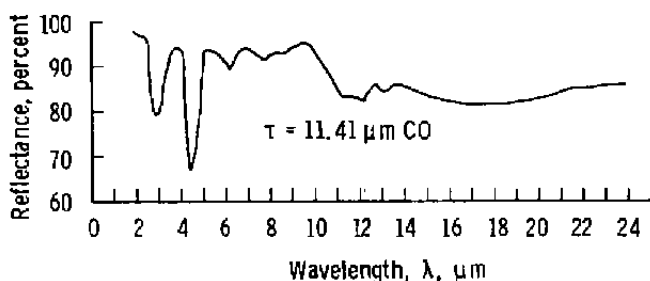
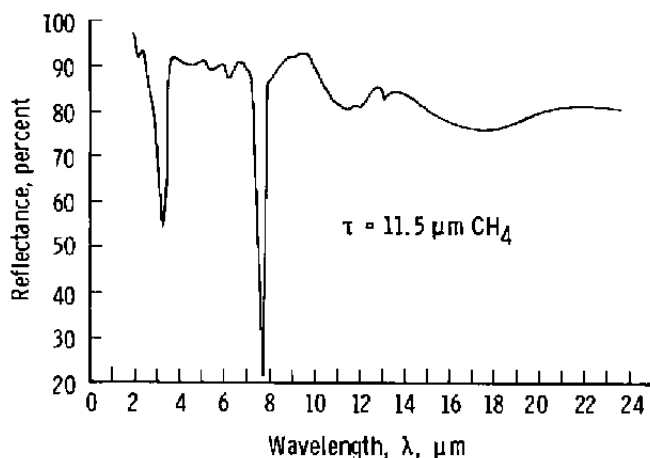


Figure 8. Reflectance of CO film on  $20^\circ\text{K}$  aluminum mirror.

### Methane ( $\text{CH}_4$ )

Methane will deposit at  $33^\circ\text{K}$  or lower for a chamber pressure of  $5 \times 10^{-8}$  torr and thus, like CO, required sample cooling with gaseous helium. The average of six measurements for solid  $\text{CH}_4$  refractive index at  $\lambda = 0.6328\text{ }\mu\text{m}$  was  $1.36 \pm 0.01$  for  $20^\circ\text{K}$ . This condensed gas gave the best quality of interference patterns of all the condensed gases investigated. Film thicknesses of up to  $41\text{ }\mu\text{m}$  (175 interference maxima) were measured by the thin-film interference technique. The reflectance of an  $11.5\text{-}\mu\text{m}$ -thick  $\text{CH}_4$  film deposited on an aluminum mirror is shown in Fig. 9. The two narrow and strong absorption bands are



**Figure 9. Reflectance of  $\text{CH}_4$  film on  $20^\circ\text{K}$  aluminum mirror.**

located at  $\lambda = 3.3$  and  $7.75 \mu\text{m}$ , which are, respectively, the  $\nu_3$  and  $\nu_4$  fundamental absorption bands.

### Nitrous Oxide ( $\text{N}_2\text{O}$ )

The spectral reflectance for condensed  $\text{N}_2\text{O}$  is shown in Fig. 10 for a film  $11.4 \mu\text{m}$  thick. It was determined from the vapor pressure curves that  $\text{N}_2\text{O}$  would condense, at a chamber pressure of  $5 \times 10^{-8}$  torr, on a  $73^\circ\text{K}$  or cooler surface, and that it thus required that the aluminum mirror sample be cooled with gaseous helium from the refrigeration system. The refractive index of solid  $\text{N}_2\text{O}$  at  $20^\circ\text{K}$  and  $\lambda = 0.6328 \mu\text{m}$  was determined to be  $1.29 \pm 0.01$  as averaged over three determinations. The strongest absorption band seen in Fig. 10 is the  $\nu_1$  band at  $\lambda = 8.85 \mu\text{m}$  with the  $\nu_2$  band at  $17.05$ , the  $\nu_3$  at  $4.5$ ,  $2\nu_2$  at  $8.55$ ,  $2\nu_1$  at  $3.85$  and the  $\nu_1 + \nu_3$  combination band at  $2.9 \mu\text{m}$ . These band locations agree quite closely with absorption bands for  $\text{N}_2\text{O}$  in the gaseous state (Ref. 15).

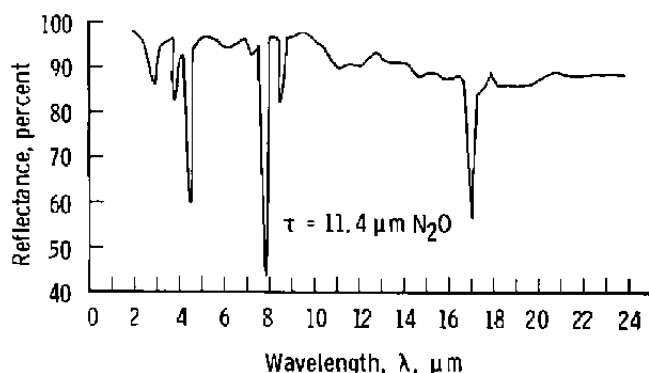


**Figure 10. Reflectance of  $\text{N}_2\text{O}$  film on  $20^\circ\text{K}$  aluminum mirror.**

## Nitric Oxide (NO)

Nitric oxide films will condense at about 50°K or lower for a chamber pressure of  $5 \times 10^{-8}$ . The spectral reflectance for an 11.4- $\mu\text{m}$ -thick film on an aluminum mirror is shown in Fig. 11 for a substrate temperature of 20°K. The solid NO refractive index (at 20°K and  $\lambda = 0.6328 \mu\text{m}$ ) averaged over nine measurements was  $1.38 \pm 0.02$ . The major absorption bands are found to occur at  $\lambda = 5.8$  and  $5.45$ , the location of the fundamental stretching mode, with weaker bands at 2.8, 7.8, 10.8, 12.8, and 17.1  $\mu\text{m}$ .

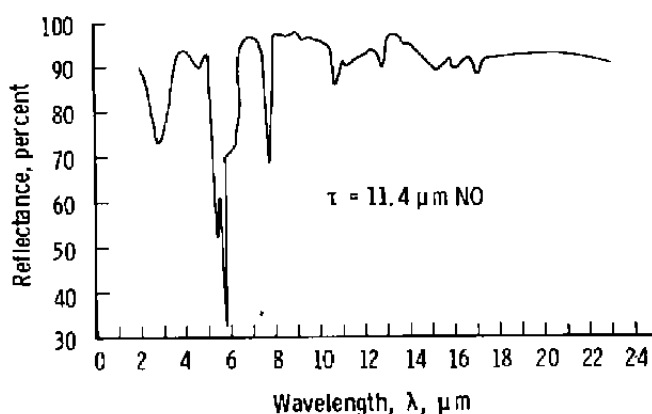
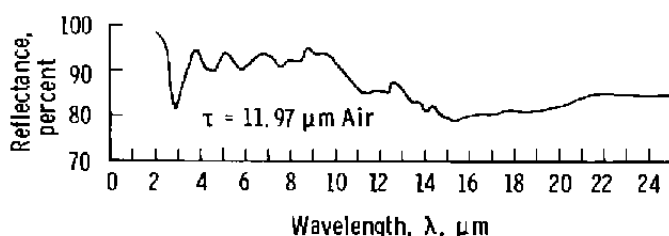


Figure 11. Reflectance of NO film on 20°K aluminum mirror.

## Air

The next gas investigated was atmospheric (or room) air. The refractive index of condensed air at 20°K and  $\lambda = 0.6328 \mu\text{m}$  was found to be  $1.28 \pm 0.01$ , which was the same value determined for pure solid  $\text{N}_2$ . The spectral reflectance for the 11.97- $\mu\text{m}$ -thick air deposit on a 20°K aluminum mirror can be observed in Fig. 12. The  $\text{H}_2\text{O}$  band at 2.9  $\mu\text{m}$  is the strongest band observed. The  $\text{CO}_2$  band at 4.3  $\mu\text{m}$  occurs in the same general location as the interference minima and is not readily apparent. Evidently, most of the deposit is  $\text{N}_2$  and  $\text{O}_2$ , which are not infrared-active;  $\text{H}_2\text{O}$  and  $\text{CO}_2$  occur only as trace amounts in the deposit. In Fig. 12, the very broad depression in the spectral reflectance between  $\lambda = 13$  and 21  $\mu\text{m}$  is believed to be due to  $\text{H}_2\text{O}$  absorption. The interference patterns observed for the 0.6328- $\mu\text{m}$  radiation were found to be of high quality; at least 125 patterns were observed before the pattern's disappearance. This indicates that the deposit is amorphous and therefore exhibits little scattering relative to that observed for crystalline films.



**Figure 12. Reflectance of condensed air film on 20°K aluminum mirror.**

### Allene ( $C_3H_4$ )

Allene, or propadiene, a compressed flammable gas, was deposited on 20- and 77°K-cooled aluminum mirrors. The refractive index of solid  $C_3H_4$  at  $\lambda = 0.6328 \mu m$  was found to be  $1.26 \pm 0.01$  and  $1.43 \pm 0.02$  at 20 and 77°K, respectively. As shown in Fig. 13 for a 20°K film  $24.8 \mu m$  thick, allene has several sharp absorption bands. The band assignments are as follows: The  $\nu_6$  band occurs at  $5.25 \mu m$ ; the  $\nu_7$  band at  $7.35 \mu m$ ; the  $\nu_9$  band at  $9.95 \mu m$ ; the strongest band,  $\nu_{10}$ , with a possible contribution of  $\nu_4$ , occurs at  $11.8 \mu m$ , and the band at  $6.05 \mu m$  is believed to be the  $2\nu_{10}$  band.

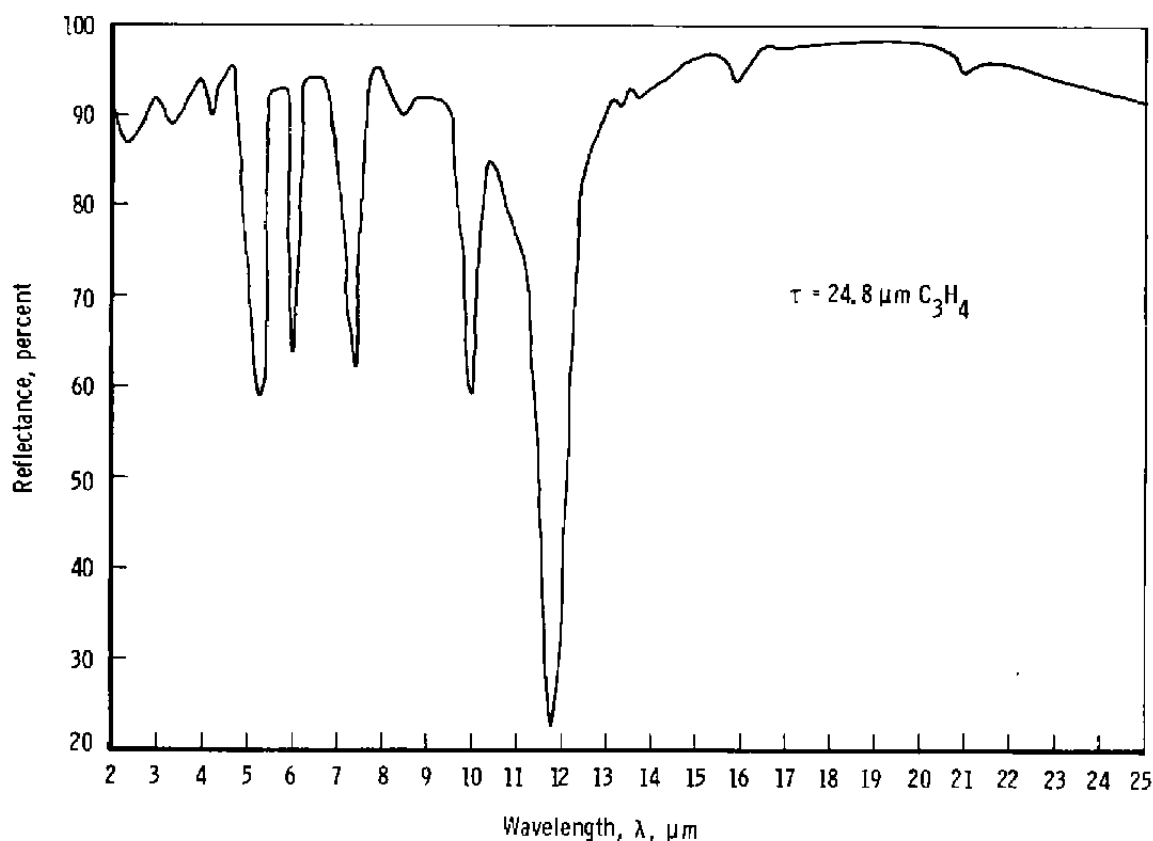


**Figure 13. Reflectance of condensed allene film on 20°K aluminum mirror.**

## 6.0 COMPARISON OF REFLECTANCE MEASUREMENTS

A comparison was sought of the reflectance measurements made in the HEMR with results obtained on the same samples at other facilities. The opportunity arose through a SAMSO-AEDC surface degradation test. Eleven anodized surfaces were investigated to determine the bidirectional reflectance of the surfaces and the hemispherical-directional reflectance. The bidirectional measurements were conducted at AEDC, and the hemispherical-directional reflectance measurements were made by General Dynamics Convair (GDC), Air Force Materials Laboratory (AFML), and AEDC in a round-robin series of tests. The reflectometer used by GDC is a system similar to the HEMR. It incorporates a hemiellipsoidal mirror of the same dimensions as the HEMR in use at AEDC but has the added capability of varying the incidence angle, and it can operate in the absolute mode as well as in the reference mode. The AFML instrument is a Fourier Transform Interferometer Spectrophotometer (Willey Model 318S) that employs a diffuse gold coated integrating sphere. The surfaces to be measured are maneuvered into place at the bottom of the integrating sphere.

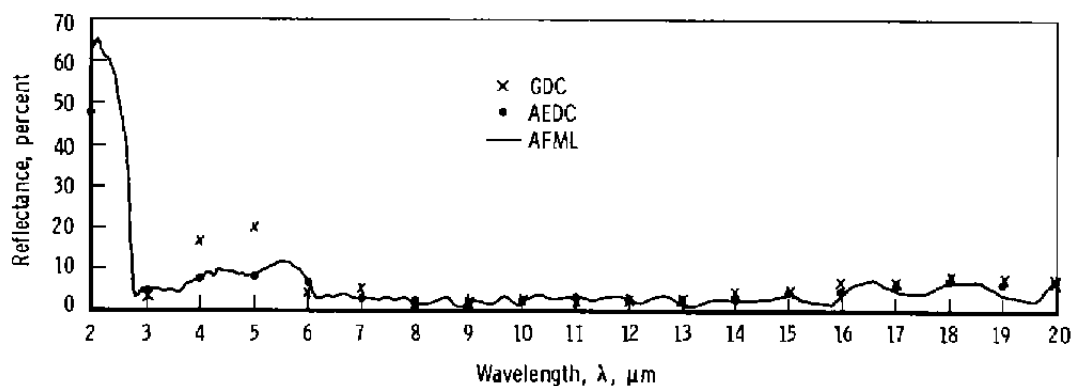
GDC was the first company to measure the reflectance of the anodized samples. The samples were prepared at the different organizations using beryllium, titanium, and aluminum. In some instances the sample was chemically etched before being anodized with sulfuric acid. The samples, listed in Table 2, were obtained by SAMSO. The reflectances measured for the various samples are shown in Figs. 14 through 25. Figures 14 through 17 are for samples that were only anodized, whereas the data in Fig. 15 are for a sample chemically etched and then anodized. Chemical etching slightly decreased the reflectance, as can be seen by comparing the results in Figs. 14 and 15 for the two Anodite, Inc., samples. The AEDC anodized sample was studied only by AEDC and AFML (see results in Fig. 17). Figures 18 and 19 show the reflectance for anodized 7075 aluminum, and Fig. 20 gives the results for 7075 aluminum that was anodized after being chemically etched. Figure 21 gives reflectance results for the Anodite, Inc., prepared aluminum 2024 that was chemically etched and anodized, and Fig. 22, the results for the Harges, Inc. aluminum 2024 that was anodized only. Figure 23 presents the reflectance data for titanium anodized by Anodite, Inc., and Fig. 24 shows the data for anodized titanium prepared by Lubeco, Inc. Figure 25 shows the reflectances measured for an anodized beryllium sample prepared by Anodite, Inc.

The agreement between the measurements of the three reflectometer systems is good. The largest disagreements were observed in Figs. 23 and 24 for the titanium samples. In contrast to the close measurement agreement obtained for the other samples, the disagreement in results for these two samples is considerable. A possible explanation for

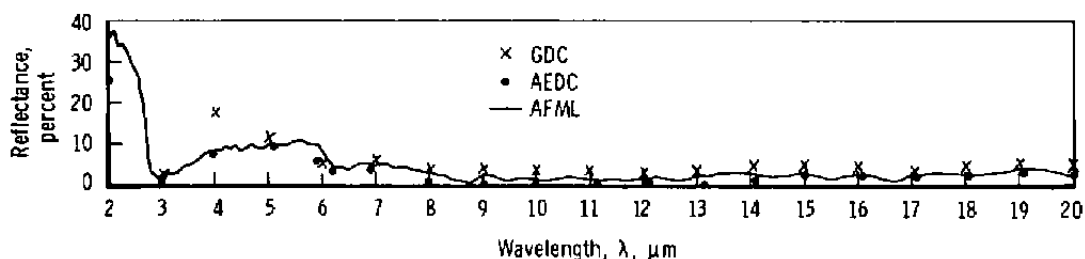


**Table 2. SAMSO Anodized Samples.**

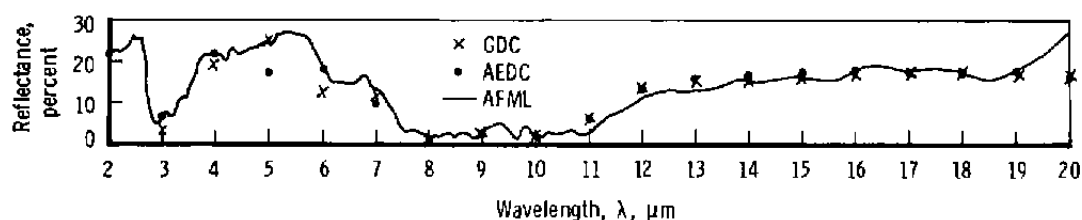
<u>Sample No.</u>	<u>Substrate Material</u>	<u>Treatment</u>	<u>Processing Company</u>
1	6061 Aluminum	H <sub>2</sub> SO <sub>4</sub> anodized	Anodite, Inc.
2	6061 Aluminum	Chemically etched and H <sub>2</sub> SO <sub>4</sub> anodized	Anodite, Inc.
3	6061 Aluminum	Anodized	Hardes, Inc.
4	6061 Aluminum	H <sub>2</sub> SO <sub>4</sub> anodized	AEDC
5	7075 Aluminum	H <sub>2</sub> SO <sub>4</sub> anodized	Anodite, Inc.
6	7075 Aluminum	Anodized	Hardes, Inc.
7	7075 Aluminum	Chemically etched and H <sub>2</sub> SO <sub>4</sub> anodized	Anodite, Inc.
8	2024 Aluminum	Chemically etched and H <sub>2</sub> SO <sub>4</sub> anodized	Anodite, Inc.
9	2024 Aluminum	Anodized	Hardes, Inc.
10	Titanium	Anodized	Anodite, Inc.
11	Titanium	Anodized	Lubeco, Inc.
12	Beryllium	Anodized	Anodite, Inc.



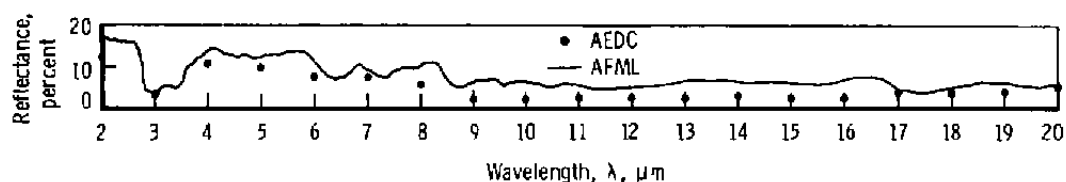
**Figure 14. Comparison of reflectance data from GDC, AFML, and AEDC for a 6061 aluminum sample that was H<sub>2</sub>SO<sub>4</sub> anodized by Anodite, Inc.**



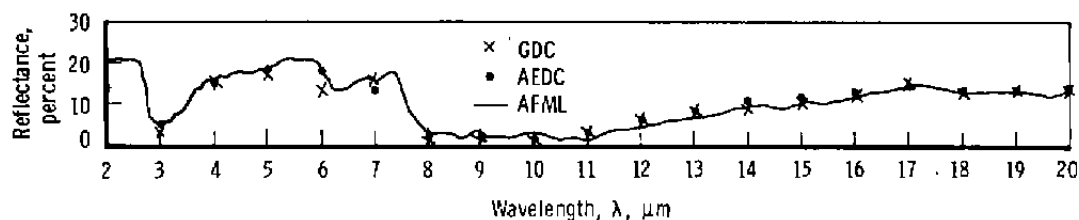
**Figure 15.** Comparison of reflectance data from GDC, AFML, and AEDC for a 6061 aluminum sample that was deep chemically etched and  $\text{H}_2\text{SO}_4$  anodized by Anodite, Inc.



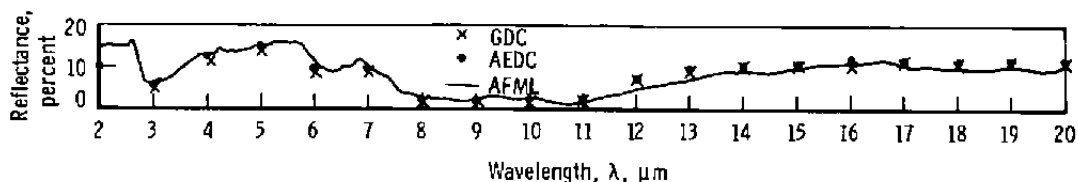
**Figure 16.** Comparison of reflectance data from GDC, AFML, and AEDC for a 6061 sample that was anodized by Harges, Inc.



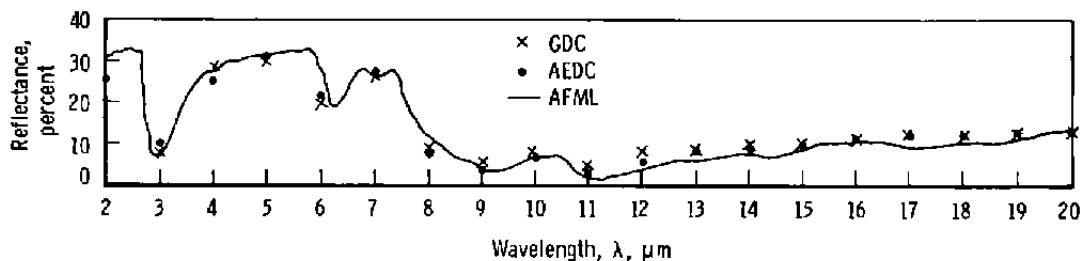
**Figure 17.** Comparison of reflectance data from AFML and AEDC for a 6061 aluminum sample that was  $\text{H}_2\text{SO}_4$  anodized at AEDC.



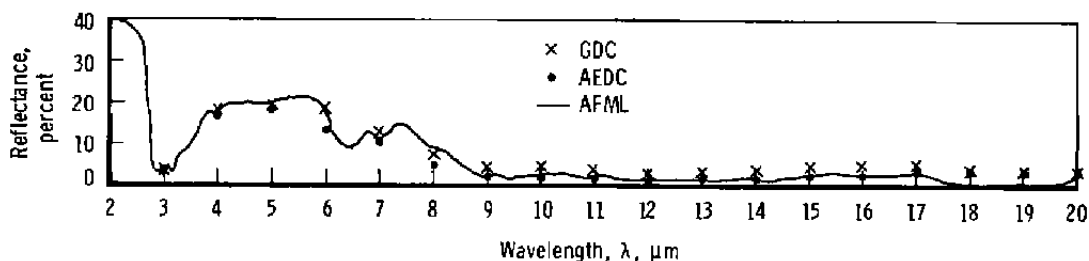
**Figure 18.** Comparison of reflectance data from GDC, AFML, and AEDC for a 7075 aluminum sample that was  $\text{H}_2\text{SO}_4$  anodized by Anodite, Inc.



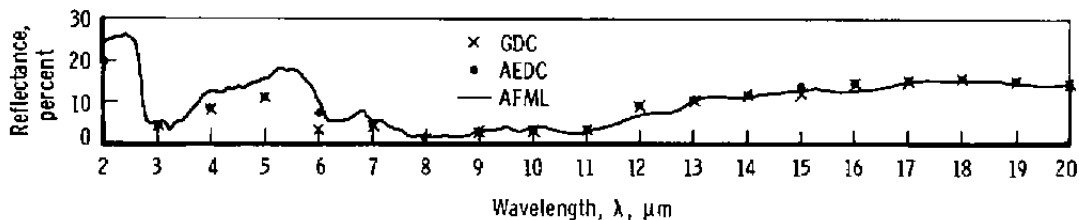
**Figure 19. Comparison of reflectance data from GDC, AFML, and AEDC for a 7075 aluminum sample that was anodized by Hardes, Inc.**



**Figure 20. Comparison of reflectance data from GDC, AFML, and AEDC for a 7075 aluminum sample that was deep chemically etched and  $H_2SO_4$  anodized by Anodite, Inc.**

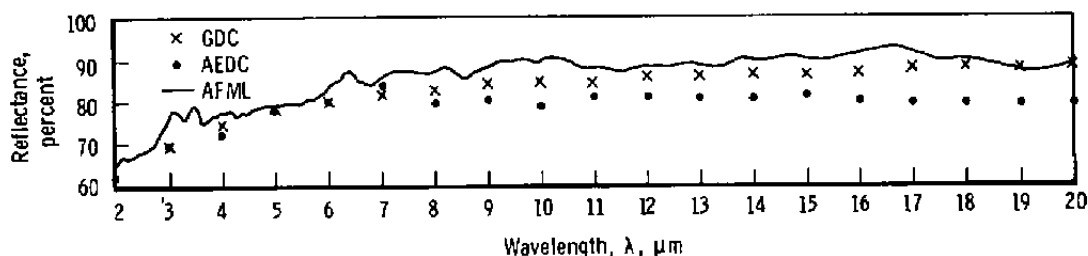


**Figure 21. Comparison of reflectance data from GDC, AFML, and AEDC for a 2024 aluminum sample that was deep chemically etched and  $H_2SO_4$  anodized by Anodite, Inc.**

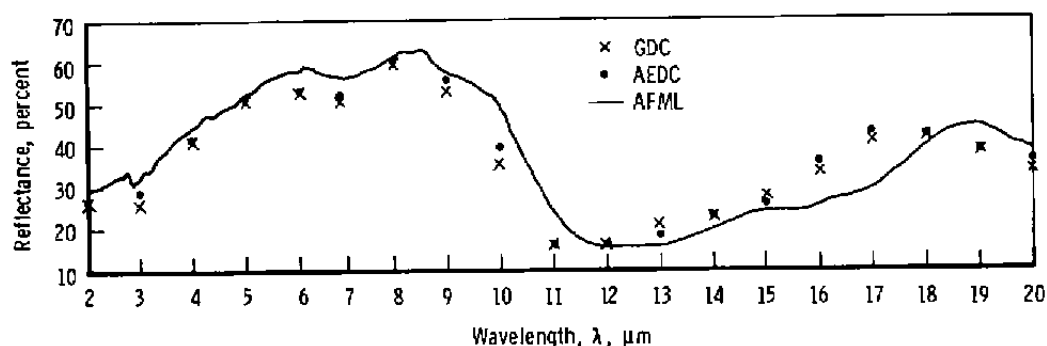


**Figure 22. Comparison of reflectance data from GDC, AFML, and AEDC for a 2024 aluminum sample that was anodized by Hardes, Inc.**

the disagreement is that the same side of these two samples may not have been measured. Both sides of these two samples appeared to be identical, but this may not have been the case in the infrared. There did not appear to be a consistent trend in the measurement disagreements: None of the three reflectometers consistently read higher or lower than the others. Examining the two figures showing the greatest disagreement in measurements — Figs. 23 and 24 — reveals that the AEDC data were considerably below the AFML and GDC data in Fig. 23, whereas the AFML data were considerably below the AEDC data for  $\lambda > 12 \mu\text{m}$  in Fig. 24. Except for these two cases the agreement between measurements of all three reflectometers was generally good, within a variation of  $\Delta R = \pm 1.5$  percent.



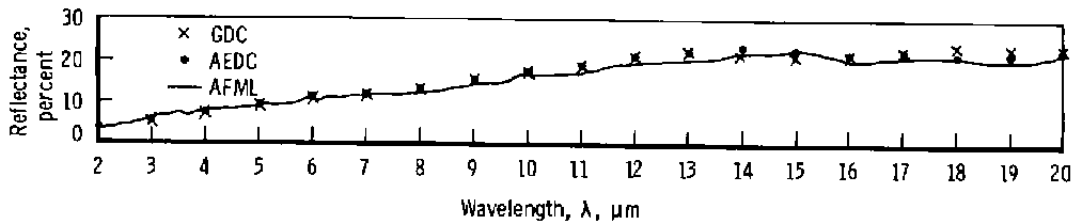
**Figure 23.** Comparison of reflectance data from GDC, AFML, and AEDC for a titanium sample that was anodized by Anodite, Inc.



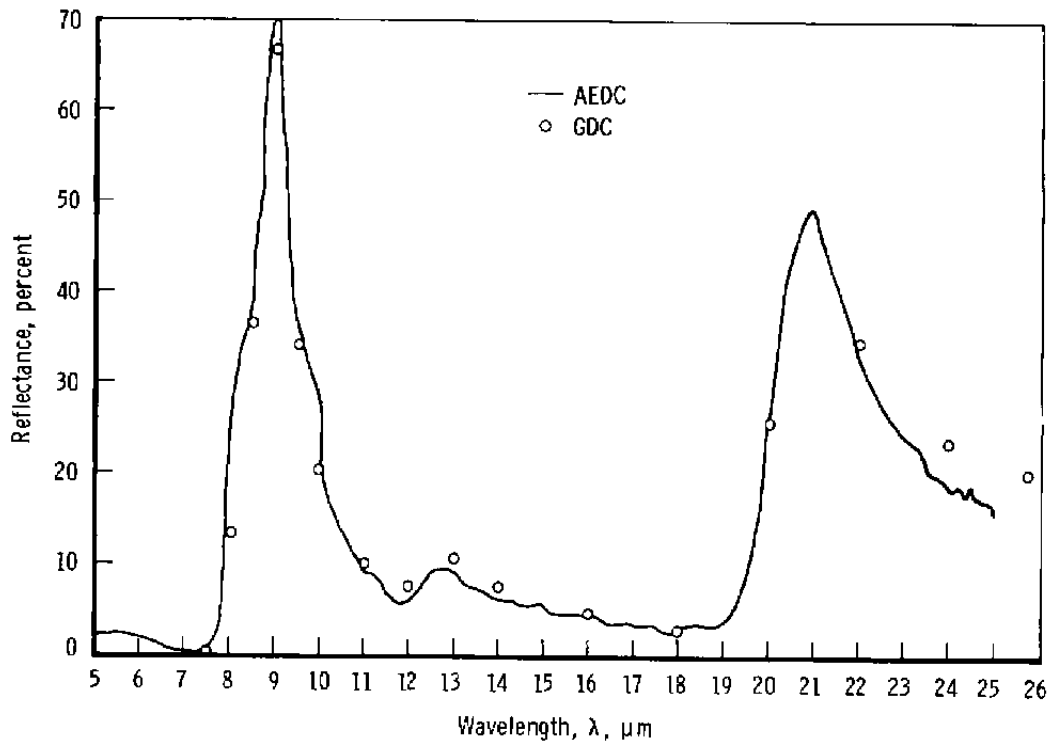
**Figure 24.** Comparison of reflectance data from GDC, AFML, and AEDC for a titanium sample that was anodized by Lubeco, Inc.

Figure 26 shows a comparison of reflectance data obtained for an Optosil I® sample in the HEMR with measurements by General Dynamics Convair (Ref. 16). This sample has a specular surface and is a type of quartz mentioned as a possible standard reference surface for reflectance. As can be seen, the two sets of measurements nearly agree. In Fig. 27, reflectance measurement comparison is made between the HEMR and NBS data (obtained

with a Cary 90 infrared reflectometer) for Bendix 1601 Krylon® flat black paint. Agreement of the measurements for this surface was excellent.



**Figure 25. Comparison of reflectance data from GDC, AFML, and AEDC for a beryllium sample that was anodized by Anodite, Inc.**



**Figure 26. Comparison of reflectance of Optosil I® measured in the HEMR at AEDC with the results of the General Dynamics Convair reflectometer.**

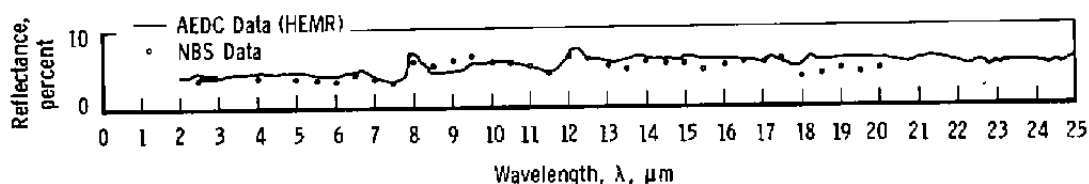


**Figure 27. Comparison of HEMR reflectance measurements for Bendix black paint sample #1601 Krylon® with those obtained at NBS.**

## 7.0 SUMMARY

Spectral reflectance and refractive index measurements have been made for twelve condensed gases:  $\text{CO}_2$ ,  $\text{H}_2\text{O}$ ,  $\text{NH}_3$ ,  $\text{CO}$ ,  $\text{CH}_4$ ,  $\text{O}_2$ ,  $\text{N}_2$ ,  $\text{A}$ ,  $\text{NO}$ ,  $\text{N}_2\text{O}$ ,  $\text{C}_3\text{H}_4$ , and air. Reflectance measurements were made only for the nine infrared active species. Neither the homonuclear gases, such as  $\text{N}_2$  and  $\text{O}_2$ , nor the atomic gas argon were studied in the IR infrared inactive. The other gases do exhibit infrared absorption, and their spectra were studied over the 2- to 25-  $\mu\text{m}$  range. Thin films of condensed gas of approximately 10  $\mu\text{m}$  thickness were vacuum deposited at  $10^{-7}$  to  $10^{-8}$  torr on aluminum-coated mirrors and their reflectance measured in the hemiellipsoidal mirror reflectometer. Refractive indices of all twelve gases were made at the He-Ne laser wavelength of 0.6328  $\mu\text{m}$ . For each of the three gases condensed on both 77 and 20°K surfaces,  $\text{CO}_2$ ,  $\text{H}_2\text{O}$ , and  $\text{NH}_3$ , the refractive index was significantly lower at the lower temperature, 20°K. From these results it is concluded that the HEMR system can be used for studies of optical properties and reflectance effects of any gaseous contaminant that will condense on cryogenically cooled optical surfaces. This includes studies on outgassing products from materials or studies on reevaporation and condensation of solid contaminants, such as rocket motor exhaust products.

From the reflectance data comparison for the SAMSO samples, generally excellent measurement agreement was obtained among the three reflectometers at General Dynamics Convair, Air Force Materials Laboratory, and AEDC. Excellent agreement was also found between the HEMR and NBS reflectance data for the one sample whose reflectance was measured. Comparisons of reflectance measurements were made for 14 samples — twelve that were anodized aluminum, beryllium, or titanium, one that was a black paint, and one that was a polished Optosil quartz sample.

## REFERENCES

1. Wood, B. E., Pipes, J. G., Smith, A.M., and Roux, J. A. "Hemi-Ellipsoidal Mirror Infrared Reflectometer: Development and Operation." *Applied Optics*, Vol. 15, No. 4, April 1976, pp. 940-950.
2. Wood, B. E., Pipes, J. G., Smith, A.M., and Roux, J. A. "Focusing Properties and Operation of a Hemiellipsoidal Mirror Infrared Reflectometer." In *Progress in Astronautics and Aeronautics: Vol. 49, Radiative Transfer and Thermal Control*, edited by A. M. Smith. American Institute of Aeronautics and Astronautics, New York, 1976, pp. 47-66.
3. Wood, B. E., Smith, A. M., Roux, J. A., and Seiber, B. A. "Spectral Absolute Reflectance of CO<sub>2</sub> Frosts from 0.5 to 12.0  $\mu$ ." *AIAA Journal*, Vol. 9, No. 7, July 1971, pp. 1338-1344.
4. Wood, B. E., Smith, A. M., Roux, J. A., and Seiber, B. A. "Spectral Infrared Reflectance of H<sub>2</sub>O Condensed on LN<sub>2</sub>-cooled Surfaces in Vacuum." *AIAA Journal*, Vol. 9, No. 9, September 1971, pp. 1836-1842.
5. Seiber, B. A., Smith, A. M., Wood, B. E., and Roux, J. A. "Solar Reflectance of Cryodeposits, Part I: H<sub>2</sub>O on LN<sub>2</sub>-cooled Black Paint." In *Progress in Astronautics and Aeronautics: Vol. 65, Thermophysics and Thermal Control*, edited by Raymond Viskanta. American Institute of Aeronautics and Astronautics, New York, 1979, pp. 47-65.
6. Seiber, B. A., Smith, A. M., Wood, B. E., and Roux, J. A. "Solar Reflectance of Cryodeposits, Part II: CO<sub>2</sub> on Black Paint and Stainless Steel." In *Progress in Astronautics and Aeronautics: Vol. 65, Thermophysics and Thermal Control*, edited by Raymond Viskanta. American Institute of Aeronautics and Astronautics, New York, 1979, pp. 66-80.
7. Arnold, Frederick, Sanderson, Richard B., Mantz, Arlan W., and Thompson, Samuel B. "Infrared Spectral Reflectance of Plume Species on Cooled Low Scatter Mirrors." AFRPL-TR-73-52 (AD777285), September 1973.
8. Smith, A. M., Tempelmeyer, K. E., Wood, B. E., and Müller, P. R., "Angular Distribution of Visible and Near IR Radiation Reflected from CO<sub>2</sub> Cryodeposits." *AIAA Journal*, Vol. 7, No. 12, December 1969, pp. 2274-2280.

9. Smith, A. M. and Wood, B. E. "Bidirectional Reflectance of Specular and Diffusing Surfaces Contaminated with CO<sub>2</sub> Cryofilms." *Progress in Astronautics and Aeronautics: Vol. 56, Thermophysics of Spacecraft and Outer Planet Entry Probes*, edited by A. M. Smith. American Institute of Aeronautics and Astronautics, New York, 1977, pp. 157-173.
10. Smith, A. M., Wood, B. E., and Fletcher, L. S. "Bidirectional Reflectance of H<sub>2</sub>O Cryofilms on Specular and Diffusing Surfaces." *AIAA Journal*, Vol. 16, No. 5, May 1978, pp. 510-515.
11. Arnold, Frederick, "Degradation of Low-Scatter Metal Mirrors by Cryodeposit Contamination." AEDC- TR-75-128 (ADB007022L), October 1975.
12. Seiber, B. A., Smith, A. M., Wood, B. E., and Müller, P. R. "Refractive Indices and Densities of CO<sub>2</sub> and H<sub>2</sub>O Cryodeposits." American Society of Mechanical Engineers, Fluids Engineering, Heat Transfer, and Lubrication Conference, Detroit, Michigan, May 1970, Paper 70-HT-33.
13. Seiber, B. A., Smith, A. M., Wood, B. E., and Müller, P. R. "Refractive Indices and Densities of H<sub>2</sub>O and CO<sub>2</sub> Films Condensed on Cryogenic Surfaces." *Applied Optics*, Vol. 10, No. 9, September 1971, pp. 2086-2089.
14. Pipes, J. G., Roux, J. A., Smith, A. M., and Scott, H. E. "Transmission of Infrared Materials and Condensed Gases at Cryogenic Temperatures." AEDC-TR-77-71 (ADA044517), September 1977.
15. Herzberg, G. *Infrared and Raman Spectra of Polyatomic Molecules*. D. Van Nostrand Company, Inc., Princeton, New Jersey, 1954.
16. Champetier, R. J. and Friese, G. J. "Use of Polished Fused Silica to Standardize Directional Polarized Emittance and Reflectance Measurements in the Infrared." SAMSO TR-74-202 (AD 786 783), August 1974.



## APPENDIX A

### REFLECTANCE MEASUREMENTS OF POSSIBLE PLANETARY SATELLITE SURFACE CONSTITUENTS

Reflectance spectra of natural materials as they occur on planets, planetary satellites, etc., are of interest to astronomers in their efforts to determine the composition of those bodies (Refs. A-1, A-2, A-3). There are few, if any, reflectance measurements available for these materials at the temperatures at which they would most probably exist, 100 to 200°K. Types of materials such as carbonates, nitrates, chlorides, and sulfates are useful in identifying soil compositions. Reflectance data are currently being studied to attempt to determine the physical makeup of two Jupiter Galilean satellites — Callisto and Io. Astronomical reflection data have been obtained and show unexplained spectral features at 3.8 and 4.1  $\mu\text{m}$ .

Reflectance spectra of several materials were measured using the HEMR to demonstrate the variety of applications of the system. Figures A-1 to A-7 show spectral reflectance curves of, respectively,  $\text{CoSO}_4 \cdot 7\text{H}_2\text{O}$ ,  $(\text{NH}_4)_2\text{SO}_4$ ,  $\text{K}_2\text{SO}_4$ ,  $\text{CuSO}_4 \cdot 5\text{H}_2\text{O}$ ,  $\text{NiSO}_4 \cdot 6\text{H}_2\text{O}$ ,  $\text{CaCO}_3$ , and  $\text{K}_2\text{CO}_3$  for samples measured under vacuum at both room temperature

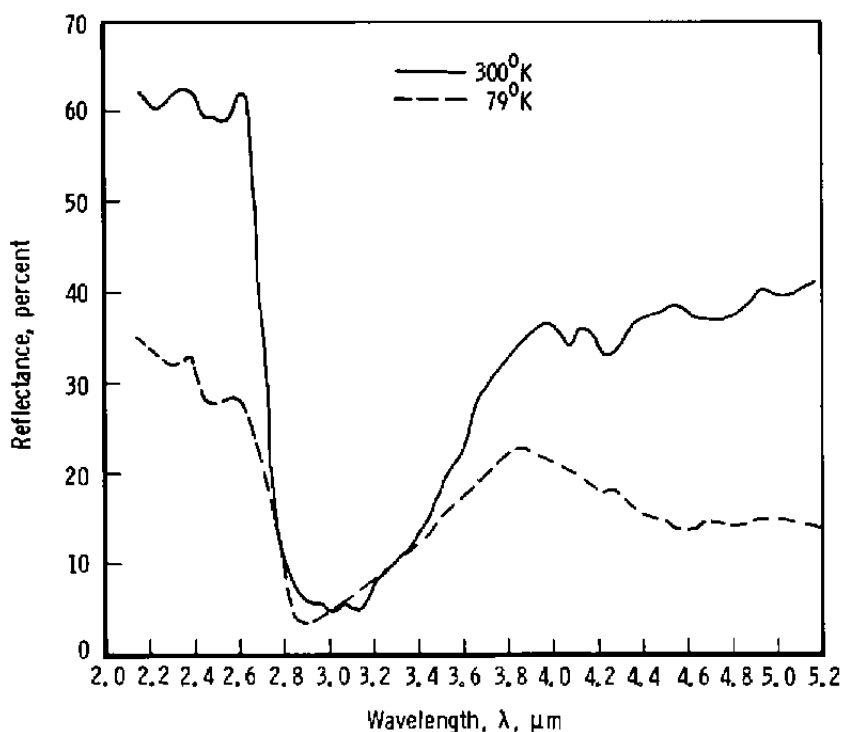


**Figure A-1. Reflectances of cobalt sulfate ( $\text{CoSO}_4 \cdot 7\text{H}_2\text{O}$ ) at 300 and 79°K.**

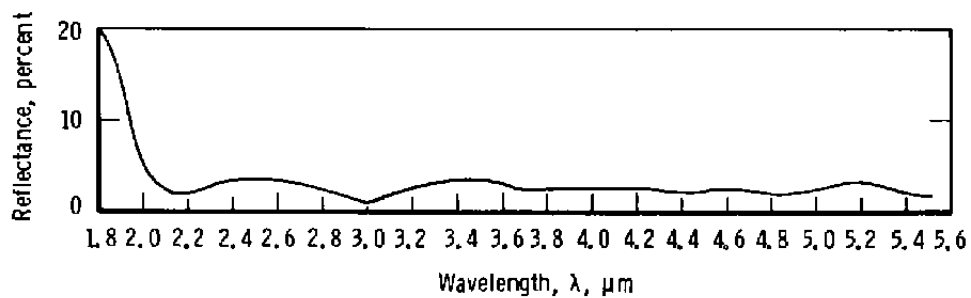


Figure A-2. Reflectance of  $(\text{NH}_4)_2\text{SO}_4$  at  $130^\circ\text{K}$ .

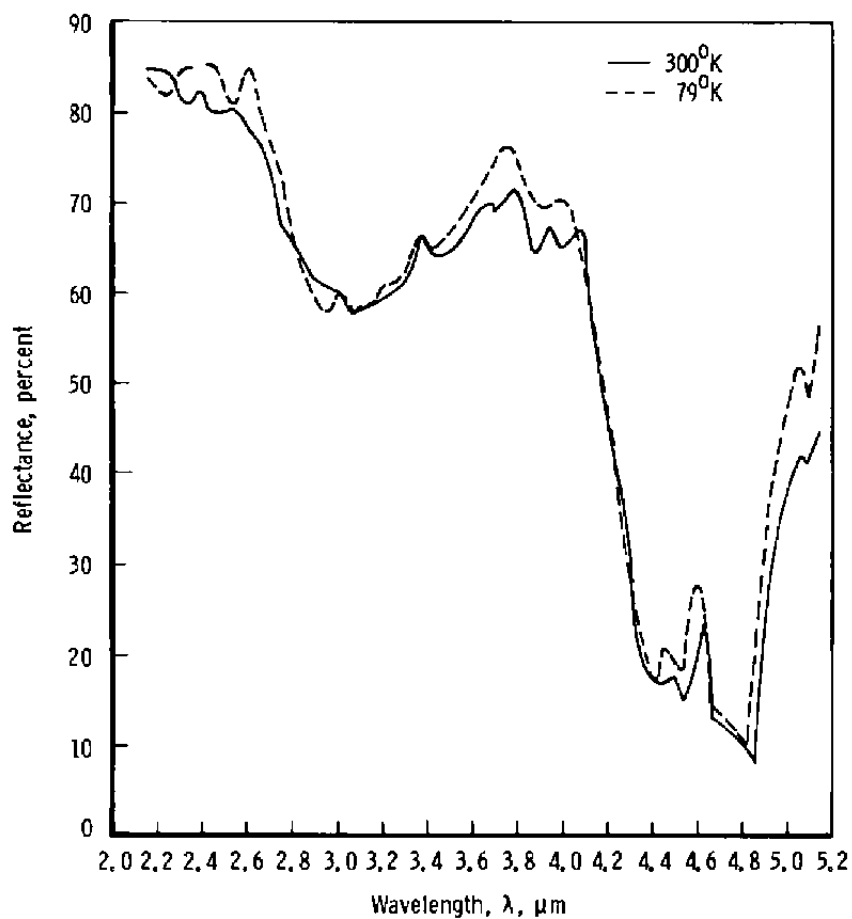


Figure A-3. Reflectances of  $\text{K}_2\text{SO}_4$  at  $300$  and  $79^\circ\text{K}$ .

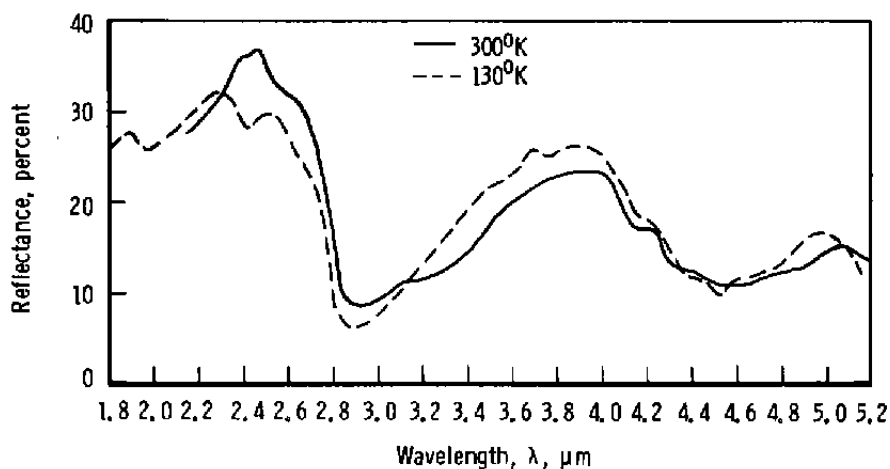


Figure A-4. Reflectances of copper sulfate ( $\text{CuSO}_4 \cdot 5\text{H}_2\text{O}$ ) at 300 and 130°K.

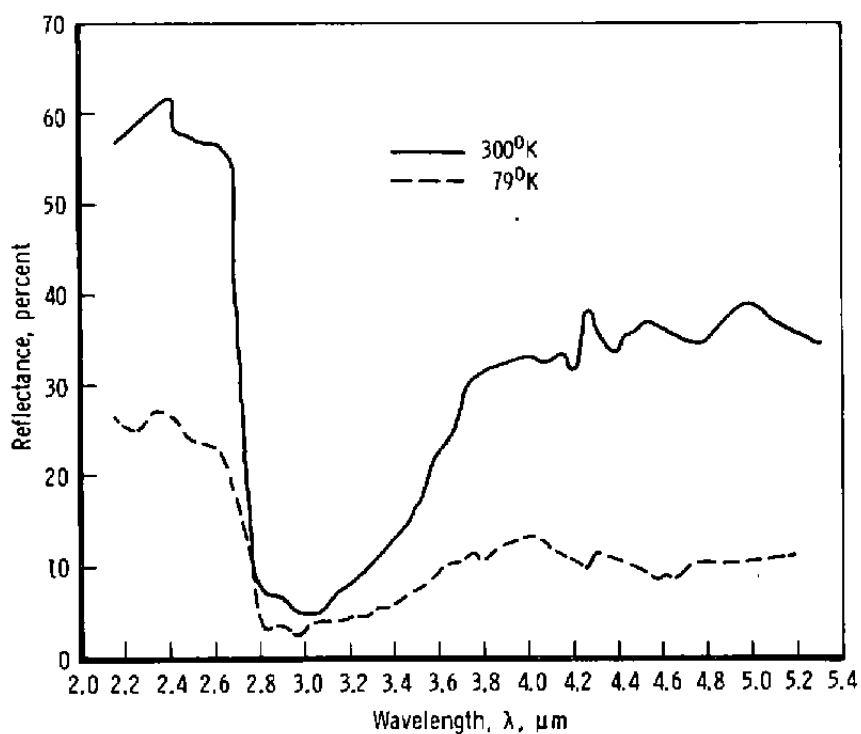
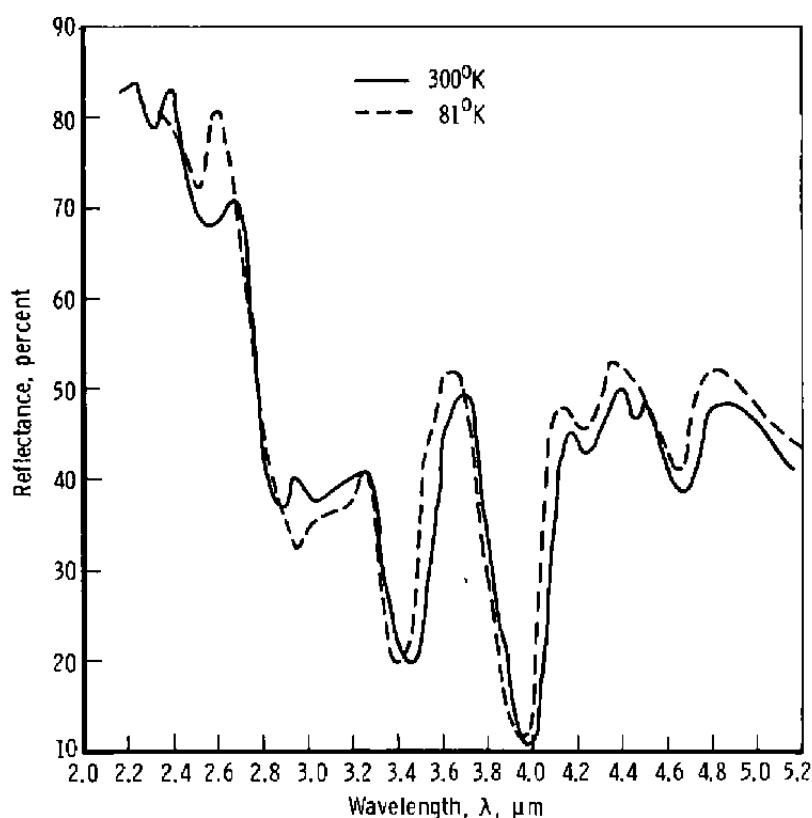


Figure A-5. Reflectances of nickel sulfate ( $\text{NiSO}_4 \cdot 6\text{H}_2\text{O}$ ) at 300 and 79°K.

( $\approx 300^\circ\text{K}$ ) and at temperatures of approximately 79 to  $130^\circ\text{K}$ . The sulfates turned brown because of their exposure to heat flux from the blackbody. However, the carbonates and  $\text{K}_2\text{SO}_4$  were not affected by this heat flux. The sulfates generally have a relatively high vapor pressure, and the chamber pressure increased from  $5 \times 10^{-6}$  torr up to about  $5 \times 10^{-5}$  torr when the samples were rotated into the reflectance measurement position at the sample focus. For reflectance measurements made at atmospheric pressure, the sulfate samples were more stable, and their appearance did not change appreciably. Under vacuum conditions the sulfate samples lost some of their water of crystallization and experienced considerable color change. The  $\text{NiSO}_4$  turned from green to yellow, the  $\text{CuSO}_4$  turned from blue to green, and the  $\text{CoSO}_4$  turned from pink to violet. No apparent shift in infrared absorption band wavelength was detected upon cooling the sample substrates to near or slightly above  $\text{LN}_2$  temperature. Because of the poor conductivity of the powdered samples, their surfaces were expected to be considerably warmer than the substrate. The general reflectance trend for the comparable samples was that the samples at room temperature were higher-reflecting than the samples at the lower temperature, especially for the cobalt sulfate and the nickel sulfate samples.



**Figure A-6. Reflectances of  $\text{CaCO}_3$  at 300 and  $81^\circ\text{K}$ .**

A mortar and pestle were used to grind up the samples, which were then packed to a thickness of 1/8 in. in a sample holder, 1 in. in diameter. For reflectance measurements the samples had to be oriented with their surfaces vertical and hence had to be tightly packed to prevent the samples' falling out. According to the data measured and presented here, only the  $K_2CO_3$  and  $CaCO_3$  exhibited absorption bands in the vicinity of  $4.1\text{ }\mu\text{m}$ . None of the materials studied exhibited any appreciable absorption at  $3.8\text{ }\mu\text{m}$ .

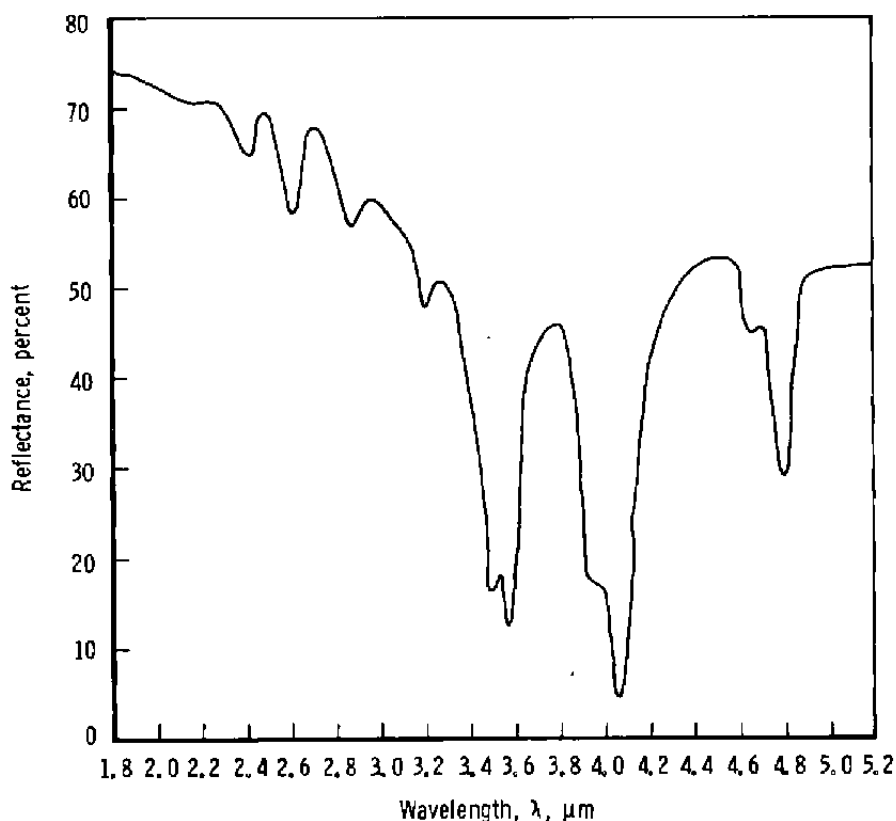


Figure A-7. Reflectance of  $K_2CO_3$  at  $130^\circ\text{K}$ .

#### REFERENCES

- A-1. Fanale, F. P., Johnson, T. V., and Matson, D. L. "Io: A Surface Evaporite Deposit?" *Science*, Vol. 186, No. 4167, 6 December 1974, pp. 922-925.
- A-2. Veverka, J. "Polarization Measurements of the Galilean Satellites of Jupiter." *Icarus*, Vol. 14, No. 3, June 1971, pp. 355-359.
- A-3. Binder, A. B. and Cruikshank, D. P. "Evidence for an Atmosphere on Io." *Icarus*, n.d., 1964, p. 299.